

Synthesis of novel vanillin derivatives: novel multi-targeted scaffold ligands against Alzheimer's Disease.

SCIPIONI, M., KAY, G., MEGSON, I.L., KONG THOO LIN, P

2019



MedChemComm

Accepted Manuscript



This article can be cited before page numbers have been issued, to do this please use: M. Scipioni, G. Kay, I. Megson and P. Kong Thoo Lin, *Med. Chem. Commun.*, 2019, DOI: 10.1039/C9MD00048H.



This is an Accepted Manuscript, which has been through the Royal Society of Chemistry peer review process and has been accepted for publication.

Accepted Manuscripts are published online shortly after acceptance, before technical editing, formatting and proof reading. Using this free service, authors can make their results available to the community, in citable form, before we publish the edited article. We will replace this Accepted Manuscript with the edited and formatted Advance Article as soon as it is available.

You can find more information about Accepted Manuscripts in the [author guidelines](#).

Please note that technical editing may introduce minor changes to the text and/or graphics, which may alter content. The journal's standard [Terms & Conditions](#) and the ethical guidelines, outlined in our [author and reviewer resource centre](#), still apply. In no event shall the Royal Society of Chemistry be held responsible for any errors or omissions in this Accepted Manuscript or any consequences arising from the use of any information it contains.

Synthesis of novel vanillin derivatives: novel multi-targeted scaffold ligands against Alzheimer's disease

MedChemComm Online
DOI: 10.1039/C9MD00048H

Matteo Scipioni¹, Graeme Kay¹, Ian L. Megson², Paul Kong Thoo Lin*¹

¹*School of Pharmacy and Life Sciences, Robert Gordon University, Aberdeen, UK*

²*Institute of Health Research & Innovation, University of the Highlands and Islands, Inverness, UK*

Abstract

Alzheimer's Disease (AD) is the most common cause of dementia worldwide, normally affecting people aged over 65. Due to the multifactorial nature of this disease, a "multi-target-directed ligands" (MTDLs) approach for the treatment of this illness has generated intense research interest in the past few years. Vanillin is a natural antioxidant and it provides a good starting point for the synthesis of new compounds with enhanced antioxidant properties, together with many biological activities, including β -amyloid peptide aggregating and acetylcholinesterase inhibiting properties. Here we report novel vanillin derivatives, bearing a tacrine or a naphthalimido moiety. All compounds exhibited improved antioxidant properties using DPPH assay, with IC_{50} as low as 19.5 μ M, FRAP and ORAC assays, with activities up to 1.54 and 6.4 Trolox equivalents, respectively. In addition, all compounds synthesized showed inhibitory activity toward acetylcholinesterase enzyme at μ molar concentrations using the Ellman assay. Computational docking studies of selected compounds showed interactions with both the catalytic anionic site and the peripheral anionic site of the enzyme. Furthermore, these compounds inhibited $A\beta_{(1-42)}$ amyloid aggregation using the fluorometric ThT assay, with compound **4** showing comparable inhibitory activity to the positive control, curcumin. At cellular level compound **4** (1 μ M) showed significant protective effects of neuroblastoma SH-SY5Y cell line when treated with hydrogen peroxide (400 μ M). In our opinion, vanillin derivatives could provide a viable platform for future development of multi-targeted ligands against AD.

Keywords: Alzheimer's Disease, Synthetic antioxidants, AChE inhibitors, Multitarget-directed ligands, Vanillin derivatives.

Introduction

Amongst all neurodegenerative diseases, Alzheimer's disease (AD) is the most common cause of dementia, mostly affecting people over the age of 65¹. In developed countries, AD is the fifth cause of death². AD is characterized by memory loss, confusion with space and time, speaking problems, poor judgment and changes in mood and personality. Due to increased life expectancy, 1 million new cases per year are expected by 2050³. For this reason, there is an urgent need for effective therapies.

AD is a multifactorial disease normally characterized by neuronal loss and β -amyloid deposition that leads to extracellular amyloid plaques in the cerebral cortex⁴. Although the cause of these events is not fully understood, the "amyloid hypothesis" is the most recognized for development of AD². More recently, oxidative injury to macromolecules, including proteins, lipids and nucleic acids has been identified as a key feature in the development of AD, thus leading to the "oxidative stress hypothesis"⁵. Finally, a decrease in acetylcholine availability at neuronal synapses is a common hallmark in AD patients², making this a possible therapeutic target.

Due to the many contributing factors involved in the development and progression of AD, the current trend of drug development based on a "one target-one molecule" point of view is no longer favored. A multi-targeted approach, aimed at targeting different steps of the neurotoxic cascade, has started to attract much interest among the research community⁶. In particular, the approach of designing multi-target agents against neurodegenerative diseases has shown an increase⁷⁻⁹. For example, recent reports include multifunctional agent chromone-2-carboxyamidoalkylbenzylamines¹⁰ and tacrine-8-hydroxyquinoline hybrids¹¹. Both groups of compounds target the cholinesterase enzymes acetylcholinesterase (AChE) and butyrylcholinesterase (BuChE), act as chelating agent with copper ion and inhibit $A\beta_{(1-42)}$ aggregation. All these events play a crucial role in the onset and progression of AD.

Multi-target compounds acting as antioxidants and acetylcholinesterase inhibitors including tacrine, a well-known acetylcholinesterase inhibitor¹² and resveratrol, a strong natural antioxidant¹³ have been recently reported¹⁴. The compounds described in this work were strong inhibitors of acetylcholinesterase (with IC_{50} at nanomolar concentrations) and $A\beta_{(1-42)}$ aggregation, while showing antioxidant activities in the 2,2-diphenyl-1-picrylhydrazyl (DPPH) assay comparable to Trolox¹⁴. Furthermore several hybrids between tacrine and Trolox, a common synthetic antioxidant, were previously reported; the compounds showed inhibitory activity toward AChE comparable to tacrine, with a two-fold decrease in the antioxidant activities in DPPH assay when compared to Trolox standard¹⁵.

Previously, we reported novel vanillin derivatives with strong antioxidant properties; in particular, compound **2c** (4,4',4'',4'''-((1,4-phenylenebis(azanetriyl))tetrakis(methylene))tetrakis(2-methoxyphenol)) exhibited remarkable scavenging activity toward DPPH free radical, as well as reducing activity in FRAP assay. In addition, the latter compound protected the SH-SY5Y neuroblastoma cell line against hydrogen peroxide (400 μ M) treatment, increasing the cell viability by 30% at compound concentrations as low as 10 μ M¹⁶.

Here we report the design and synthesis of four novel vanillin derivatives with multi-target functionalities that would be expected to exhibit antioxidant properties, as well as inhibitory AChE and amyloid $A\beta_{(1-42)}$ aggregation activities (Figure 1). Among the vanillin derivatives synthesized, three contained a naphthalimido moiety and one has a tacrine group. It is noteworthy to mention previous work reporting a naphthalimido moieties linked with ranitidine to produce potential multi-targeted AD agents¹⁷. The antioxidant properties, inhibitory AChE activity and β -amyloid aggregation inhibitory properties and their protective effect on peroxide-treated neuroblastoma SH-SY5Y cells of all the compounds synthesized in this work will be discussed.

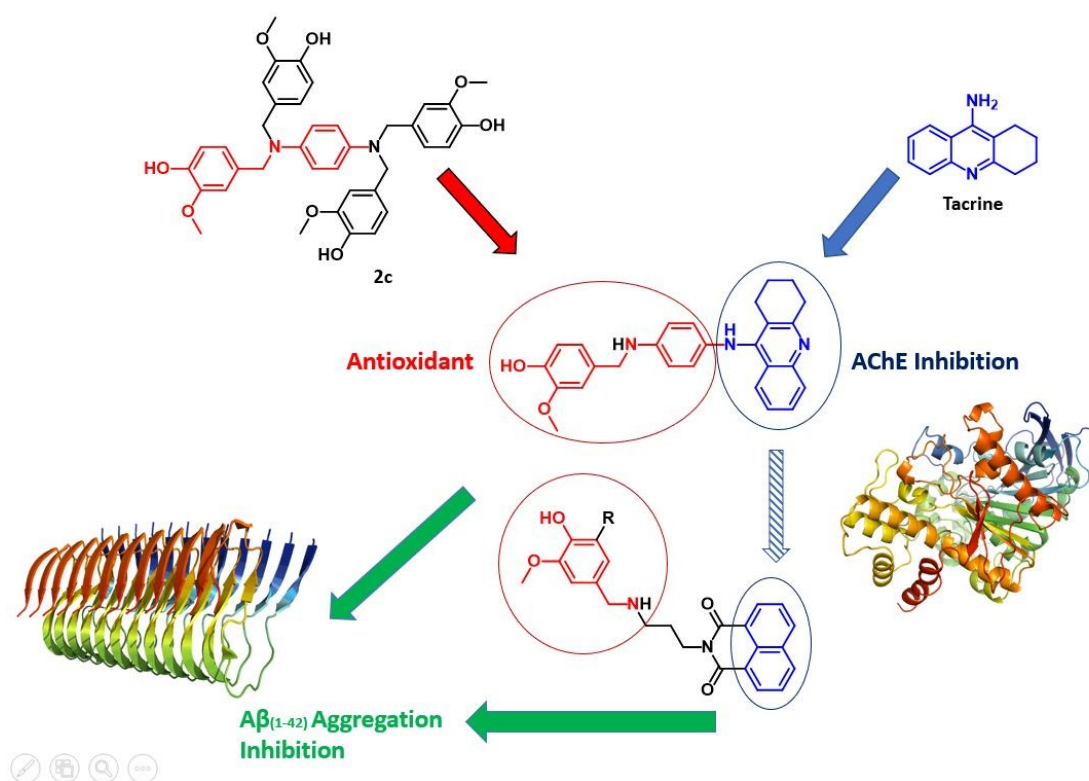


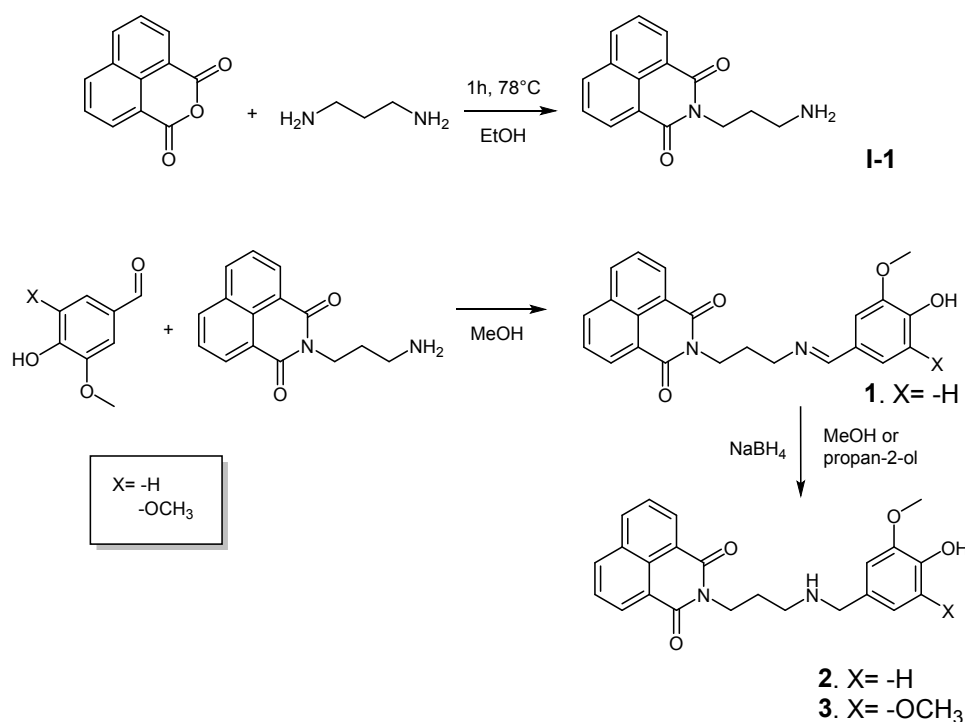
Figure 1. Rationale for the synthesis of vanillin derivatives^{18,19}.

The phenolic moiety, important for the antioxidant activity, was linked to the tacrine moiety, a well-known AChE inhibitor. Tacrine was substituted with a naphthalimido structure to determine the impact of the latter on AChE and β -amyloid inhibitory activity. In addition, the aromatic linker was substituted with a propyl moiety, which shows similar distance between the two nitrogens (5.2 and 4.9 Å, respectively, calculated using PyMOL software) and more flexibility for the evaluation of its impact on AChE and amyloid $A\beta_{(1-42)}$ peptide inhibitory activities.

Results and discussion

Chemical Synthesis

The synthesis of novel naphthalimido vanillin derivatives **1**, **2**, and **3** was achieved as depicted in Scheme 1 using 2-(3-aminopropyl)-1H-benzo[de]isoquinoline-1,3(2H)-dione (**I-1**) as a precursor. The latter was synthesised from the reaction between naphthalic anhydride and 1,3-diamino propane in ethanol according to previous work²⁰. Vanillin derivatives (**1**, **2**, and **3**) were then prepared by reacting vanillin or syringaldehyde with **I-1** to afford the corresponding imines. The latter were then reduced in the presence of sodium borohydride in methanol (**2**, 86%) or propan-2-ol (**3**, 38%).



Scheme 1. Chemical strategy for the synthesis of derivatives 1-3.

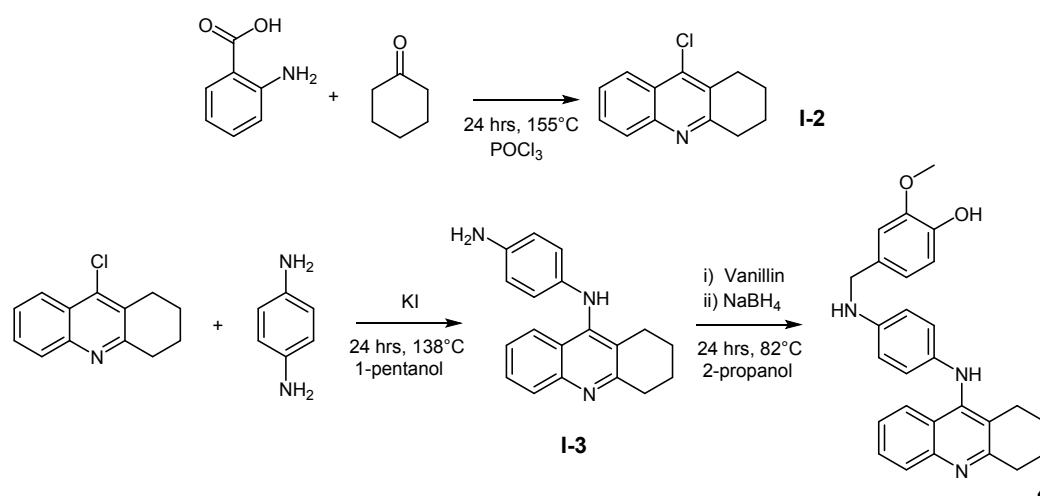
The naphthalimido compounds (**1**, **2**, **3**) showed characteristic features in their ¹H NMR spectra. The latter showed three sets of peaks between 8.65 and 7.74 ppm due to the benzo[de]isoquinoline-1,3-dione (naphthalimido) moiety along with two sets of peaks or a singlet between 7.01 and 6.50 ppm attributed to the vanillin or the syringaldehyde moieties, respectively. A singlet between 3.9 and 3.7 ppm is due to the methoxy group (in both vanillin and syringaldehyde structures) and the methylene (Ar-CH₂-N) group respectively. The propyl groups in both compounds were identified by the presence of two triplets and a multiplet between 4.4 and 1.9 ppm.

The reduction of compound **1**, to generate compound **2**, was confirmed by the disappearance of the singlet at 8.2 ppm with the appearance of new singlet (CH₂) at 3.76 ppm.

View Article Online
DOI: 10.1039/C9MD00048H

The presence of an extra methoxy group in compound **3** compared to compound **2** was also confirmed by the integration of the peak at 3.79 ppm (6 protons instead of 3).

The synthesis of compound **4** (Scheme 2) involved intermediates **I-2** and **I-3**. Compound **I-2** (67% yield) was prepared following the procedure described by Szymański, Zurek and Mikiciuk-Olasik, by reacting anthranilic acid with 2 equivalents of cyclohexanone in POCl₃ (7.5mL)²¹. Intermediate **I-3** (39 % yield) was synthesized by the N-alkylation reaction between **I-2** and of 2.5 equivalents of *p*-phenylenediamine in 1-pentanol in the presence of catalytic amount of potassium iodide (KI).



Scheme 2. Chemical strategy for the synthesis of derivative **4**.

The ¹H NMR spectrum of compound **4** showed seven sets of peaks in the region between 7.6 and 6.5 ppm attributed to the aromatic protons of the tacrine, *p*-phenylenediamine and phenolic rings. Two multiplets and two triplets between 2.6 and 1.8 ppm of the tetrahydroacridine motif from the tacrine ring system and the singlet at 3.8 ppm were due to the methoxy group from the phenolic moiety. (See experimental section and **Supplementary Information, SI**).

Antioxidant Activity

All compounds were evaluated for their antioxidant properties using three different assays (DPPH, FRAP and ORAC) with differing oxidative potential evaluating mechanisms (Table 1). DPPH assay was employed to evaluate the scavenging activity²² of the novel vanillin derivatives whereas FRAP assay was selected in order to measure the electron transfer properties²³ of the latter. Finally, the

ORAC assay was utilized for the evaluation of the hydrogen atom transfer (HAT) abilities of our novel compounds emulating a more relevant environment to biological system²⁴.

Table 1. Antioxidant properties of vanillin derivatives.

Compound	DPPH (IC ₅₀ μM)	FRAP (TE)	ORAC (TE)
1	> 250 μM	0.07 ± 0.002	2.1 ± 0.5
2	50.7 ± 0.8	0.26 ± 0.04	3.9 ± 1.3
3	19.5 ± 0.3	1.45 ± 0.02	2.0 ± 0.5
4	20.5 ± 0.3	1.54 ± 0.15	6.4 ± 1.6
Trolox	24.4 ± 0.9	1	1
Tacrine	Inactive ^a	Inactive ^a	<0.01 ^b

Results from each assay are expressed as a mean ± SD of three independent experiments.

^a Compounds were tested up to 250 μM. Trolox was used as a positive control

^b Reported by²⁵.

2,2-diphenyl-1-picrylhydrazyl (DPPH) Assay

Diphenyl-1-picrylhydrazyl (DPPH) is a stable organic nitrogen radical with an absorption maximum at 515 nm. Its reduction in the presence of antioxidants, acting as free radical scavengers, was monitored spectrophotometrically²². The IC₅₀ value of each compound was determined (see Table 1). The imine compound **1** showed no IC₅₀ up to concentration of 250 μM whereas its corresponding reduced amine showed an IC₅₀ of 50.7 μM, confirming our previous finding that an imine exhibits lower activity in free radical scavenging compared with the corresponding amine¹⁶. In addition, compound **3**, bearing an extra methoxy group in the phenolic moiety compared to compound **2**, turned out to be ~two-fold more active (19.5 μM), confirming the important role of an extra methoxy group for the antioxidant activity. Interestingly, compound **4** showed similar activity to compound **3**, although bearing only one methoxy group in its phenolic moiety (20.5 and 19.5 μM, respectively). This confirms our previous finding regarding the increase of antioxidant activity due to the electronic conjugation between the two nitrogens and an aromatic ring.

The compounds showed greater antioxidant activities compared to the tacrine-resveratrol hybrids reported by Jeřábek *et al.* which showed weak DPPH scavenging abilities due to the absence of phenolic moieties in their chemical structures ¹⁴.

Interestingly, tacrine turned out to be completely inactive at concentrations as high as 250 μM , despite the fact it has a nitrogen atom linked with an aromatic moiety. The lack of activity can be explained by the absence of a phenolic moiety in the aromatic structure.

Ferric Reducing Antioxidant Power (FRAP) Assay

The FRAP assay is based on the reduction of the ferric-tripyridyltriazine complex by antioxidants and it was performed at pH 3.5. The ferrous-tripyridyltriazine complex that is formed after the reduction of the iron core leads to a measurable blue color (593 nm) ²³. The results are expressed as Trolox Equivalent (TE) after comparison with the standard Trolox calibration curve. Again, compound **1** showed the lowest activity (0.07 TE) (see table 1), almost 15 times less active than the standard Trolox. Its reduced derivative, compound **2**, was almost 4 times less active than Trolox (0.26 TE), showing better performance compared to the corresponding imine (compound **1**). In contrast, compound **3** showed a 5-fold increase in activity (1.45 TE) compared to compound **2** confirming the importance of the extra methoxy group in the phenolic moiety for improved activity in the FRAP assay. Compound **4** turned out to be the most active among the four vanillin derivatives (1.54 TE), confirming the role of the electronic delocalisation of the nitrogen electron in the antioxidant activity ¹⁶. Again, tacrine on its own showed to be completely inactive in this assay at concentrations as high as 250 μM .

Oxygen Radical Absorbance Capacity (ORAC) Assay

ORAC assay is based on hydrogen atom transfer (HAT) mechanism and measures the ability of antioxidants to inhibit the oxidation of the fluorescent probe fluorescein caused by peroxy free radical generated by thermal decomposition of the 2,2'-azobis(2-amidinopropane) (AAPH) ²⁶⁻²⁸. The use of peroxy free radical, which is commonly found in the body, makes this assay more relevant to biological systems ²⁴.

All the novel vanillin derivatives showed improved antioxidant activities in this assay compared to the standard Trolox. Unlike the previous assays, the vanillin derivative **2** showed better activity compared to its corresponding syringaldehyde derivative **3** (3.9 and 2.0 TE, respectively) highlighting the deleterious impact of the extra methoxy moiety in the phenolic ring on ORAC assay. It is worth mentioning that vanillin itself is more active than syringaldehyde in this assay (2.2 and 1.5 TE, respectively) ¹⁶.

The imine **1** showed weaker scavenging activity compared to the amine **2** (2.1 and 3.9 TE, respectively) in this assay, confirming the role of the nitrogen's electron availability in the antioxidant activity.

Finally, compound **4** showed the highest ORAC value (6.4 TE) highlighting the predominant role of electronic delocalisation in the peroxy free radical scavenging activity.

The latter showed higher activities compared to the series of melatonin-tacrine hybrid reported by Rodriguez-Franco *et al.*, which ORAC values were ranging from 1.7 - 4.0 TE ²⁵.

Cellular Protection

View Article Online
DOI: 10.1039/C9MD00048H

MTT Assay

The production of reactive oxygen species is linked with cell death and it is a peculiar hallmark of many age-related diseases²⁹. Based on all the above results, derivative **4** was found to be the most active compound with regard to antioxidant properties. Therefore, the latter was chosen to study its ability to protect stressed cells. Neuroblastoma SH-SY5Y cell line was used for this purpose and the cell viability was determined spectrophotometrically using 3-[4,5-dimethylthiazol-2-yl]-2,5 diphenyl tetrazolium bromide (MTT) assay. Hydrogen peroxide was used as a stressor to evaluate the protective effect of compound **4** against oxidative damage; cells were exposed for 24 hours with hydrogen peroxide (400 μ M) after pre-treatment (24 hours) with compound **4** at different concentrations, ranging from 0.01 to 5 μ M.

The choice of the working concentration in the protective effect of compound **4** was based on its toxicity, after 24 hours, exposure towards SH-SY5Y neuroblastoma cell line. Compound **4** exhibited an IC_{50} of 45.1 ± 3.5 μ M, although some toxic effect was observed at concentration of 25 μ M. No significant toxicity was however found at 12.5 μ M, hence the decision to work with 5 μ M which is significantly below the toxic concentrations (see Figure 2). Compound **4** showed strong protective effect against oxidative insult and the results are reported in Figure 2.

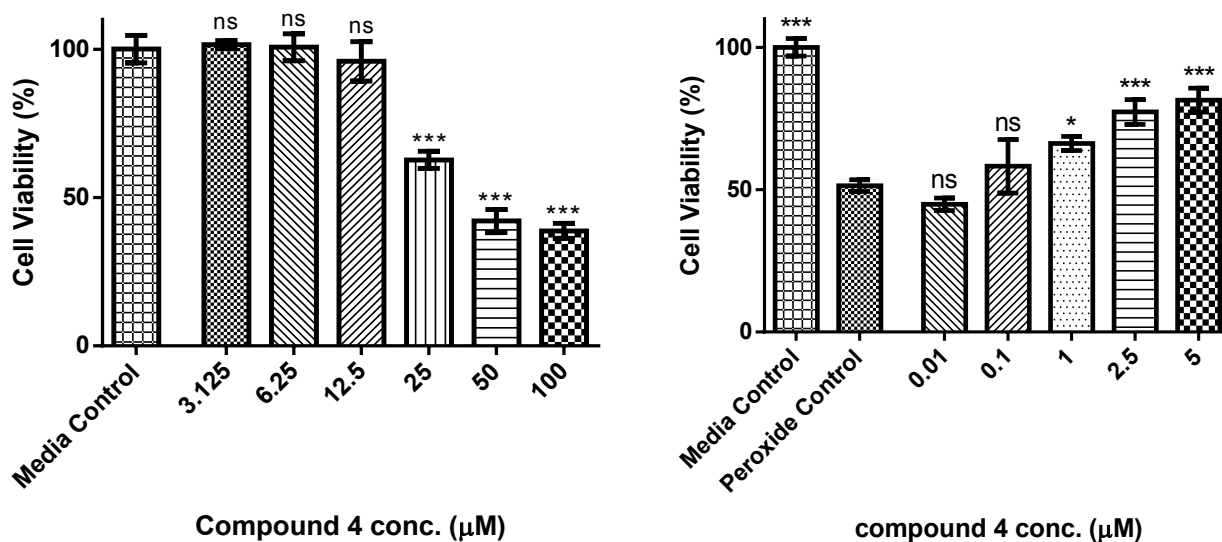


Figure 2. (Left) Toxicity of Compound **4** toward SH-SY5Y cells after 24 hours exposure. (Right) Protective effects of Compound **4** in hydrogen peroxide (400 μ M)- stressed cells. Cells were incubated for 24 hours with compound **4** at different concentrations before the addition of the stressor. After 24 hours, cell viability was measured through MTT assay. Values are expressed as the percentage of the untreated control and represented as mean \pm SD of three independent experiments in each group. *** p < 0.001, ** p < 0.01, * p < 0.05, ns no significantly different compared to the control.

Compound **4** almost completely reversed peroxide-induced cell death at the highest concentration tested (5 μM); significant protection was seen at concentrations as low as 1 μM .

No statistical protection was observed by the compound at the lowest concentrations tested (0.01 and 0.1 μM).

It is worth noting that the protective effects of compound **4** are comparable to our previously reported compound **2c**, which showed an increase in peroxide-treated cell viability by 26% at 5 μM , although **2c** showed better antioxidant properties in both the DPPH, FRAP and ORAC assays ¹⁶.

AChE Inhibitory Activity

All the compounds were evaluated for their AChE inhibition properties according to Ellman's method with minor modifications ³⁰. Tacrine was used as reference standard and the results are reported in table 2.

Table 2. Cholinesterase AChE inhibitory activity of vanillin derivatives.

Compound	AChE inhibition (IC ₅₀ μM)
1	128.3 \pm 6.1
2	10.1 \pm 1.15
3	24.25 \pm 1.35
4	2.13 \pm 0.1
Tacrine	0.93 \pm 0.09

Results are expressed as a mean \pm SD of three independent experiments.

All compounds tested showed weak to good inhibitory activity, with compound **4** the most active, with an IC₅₀ value \sim 2 times higher than the standard tacrine (IC₅₀ of 2.13 and 0.93 μM , respectively). The results obtained here for the positive control tacrine agree with the data previously reported (IC₅₀ value of 0.9 μM for tacrine) ³¹. However, compound **4** showed lower activity compared to related tacrine derivatives reported by Luo *et al.* which turned out to be several fold-times more active than tacrine ³². This could be explained by the presence of long alkyl chains in the compounds reported by the authors, which show great flexibility and adaptability within the narrow gorge of AChE compared to compound **4** that shows lower flexibility, on account of the aromatic ring linked to the tacrine moiety. The imine derivative (compound **1**) was found to

be the weakest inhibitor, with an IC_{50} of 128.3 μM . By contrast, its reduced form (compound **2**) showed an increase in activity of 13-fold (IC_{50} of 10.1 μM). This could be explained by the fact that compound **1**, which bears an imino group, will show less flexibility compared to compound **2** (amine) due to the rigidity of the double bond, thus showing reduced flexibility in the narrow gorge of the AChE enzyme. Finally, the presence of an extra methoxy group in the phenolic moiety, as in the case of compound **3**, caused a two times fold reduction in the AChE inhibition when compared with compound **2** (24.25 and 10.1 μM , respectively).

Molecular Modelling

To understand better the molecular elements that contribute to the AChE inhibitory activities of these vanillin derivatives, molecular binding studies of compounds **2** and **4** with TcAChE (PDB code: 2CMF)³³ were performed. Several studies reported the crystal structure of AChE from Torpedo Californica. The active site lies at the bottom of a 20 Å deep gorge and it is characterized by the presence of three main residues (SER-200, GLU-327, and HIS-440), which form the esteratic site involved in the hydrolysis of acetylcholine, and a catalytic anionic site (CAS), characterized by the presence of TRP-84, which plays a fundamental role in binding the acetylcholine molecule through a cation- π interaction with its positive quaternary nitrogen³⁴, and PHE-330³⁵. Finally, the peripheral anionic site (PAS) lies at the top of the gorge, approximately 20 Å above the active site. The PAS is involved in binding acetylcholine at the first step of the catalytic pathway. It is composed of residues TYR-70, ASP-72, TYR-121, TRP-279, and TYR-334³⁶.

Ligand optimization was performed using Chemdraw 16.0 (Cambridgesoft, Waltham, MA) and Chem3D Ultra 16 version (Cambridgesoft, Waltham, MA) using a MM2 force field energy minimization tool. Protein optimization was performed using Autodock Vina 1.1.2³⁷. The results were then visualized using PyMOL (the PyMOL Molecular Graphics System, Version 2.0.7 Schrödinger, LLC).

For the validation of the docking model, the original ligand in the 2CMF structure was redocked. The binding energy obtained was -14.6 kcal/mol, indicating high affinity of the latter for the AChE molecule. In addition, the comparison of the positions of the original and redocked ligands resulted in a RMSD score of 0.598 (see Figure 3), confirming the effectiveness of the Autodock Vina software.

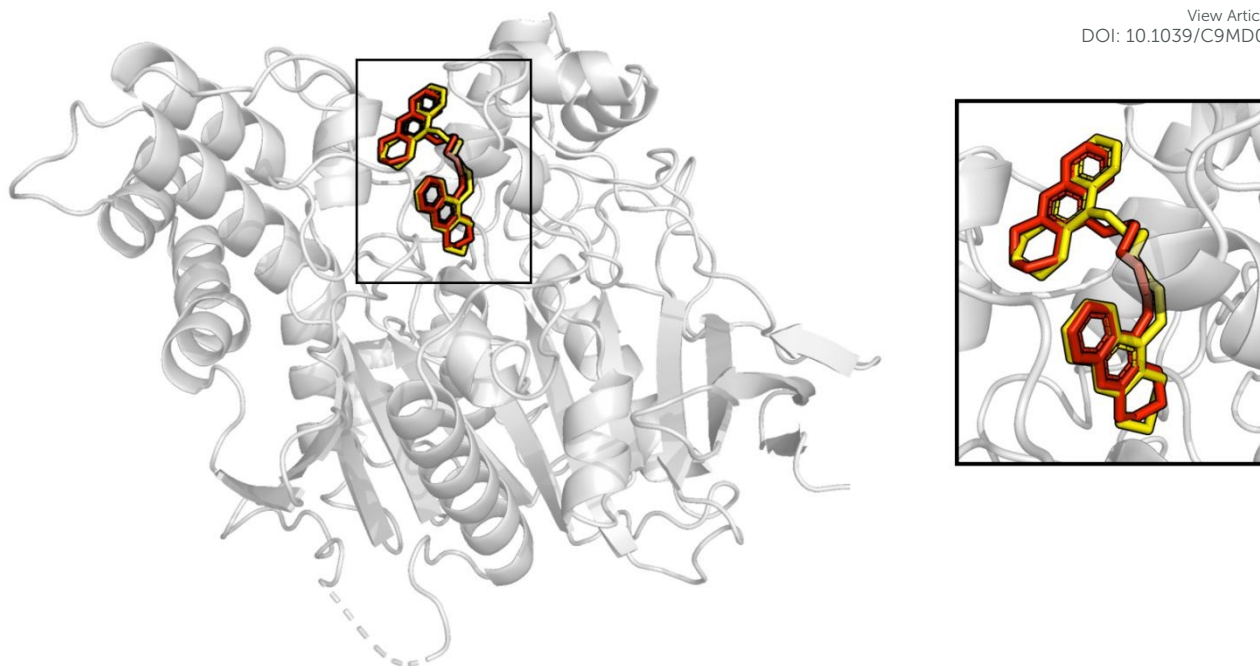


Figure 3. Redocking of the bis-tacrine derivative in *Torpedo Californica* AChE (2CMF) for the docking validation; in yellow, the ligand from the original crystal and in red, the ligand generated by redocking.

The binding scores for compounds **2** and **4** were -12.0 and -13.3 kcal/mol, respectively, matching the *in vitro* results obtained in the Ellman assay with the highest AChE inhibitory activity displayed by compound **4**. Figure 4 shows the interactions of compound **2** and **4** within the gorge of the enzyme.

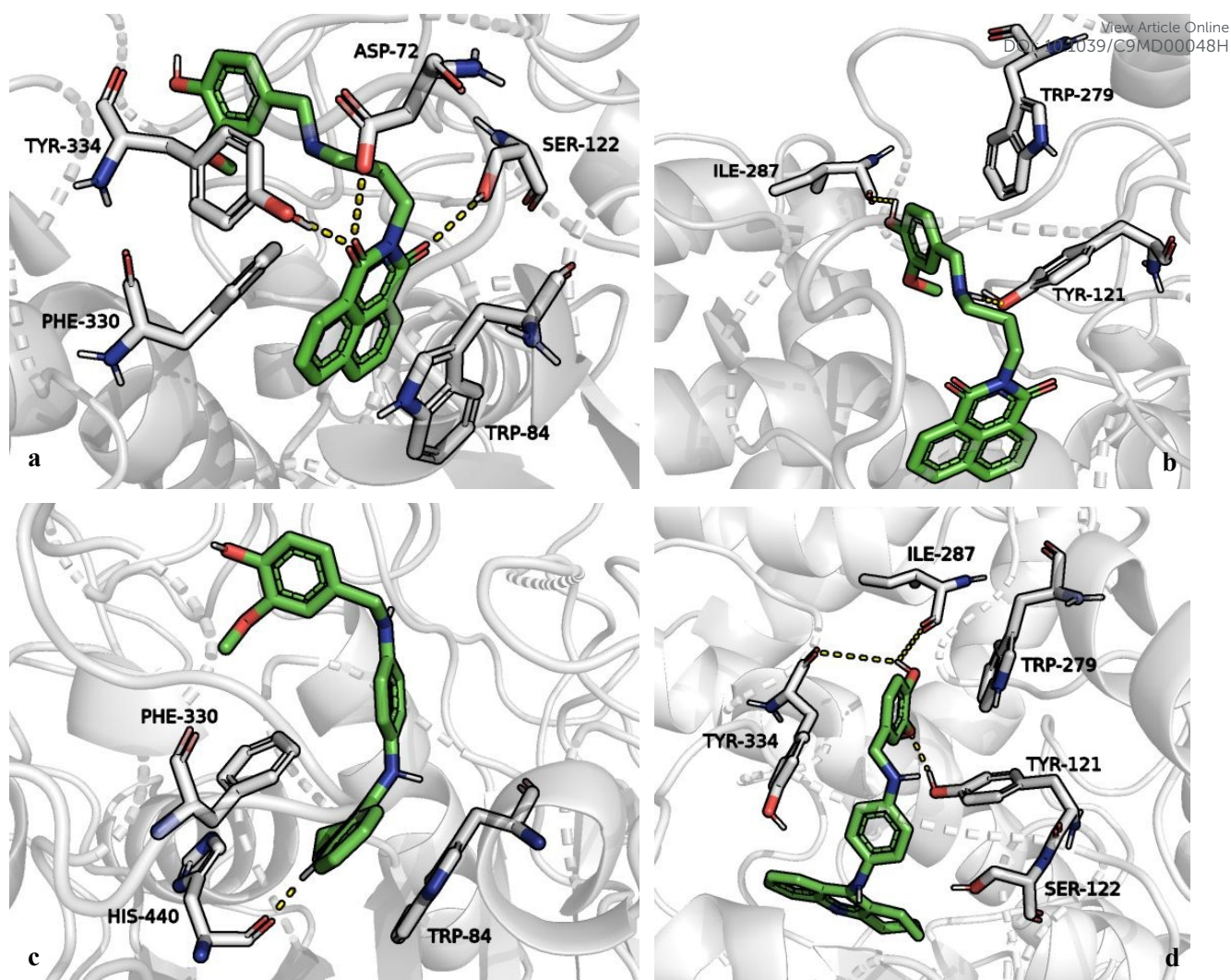


Figure 4. Predicted binding model of compounds **2** (a and b) and **4** (c and d) within the Acetylcholinesterase gorge. Compounds **2** and **4** are in green sticks whereas the amino acids involved in the interactions are in grey. Hydrogen bonds are shown as yellow dashed lines. In both models, the aromatic moieties of the compounds are stacked between the residues PHE-330 and TRP-84 (a and c). The two carbonyl groups from compound **2** form hydrogen bonds with the residues ASP-72, TYR-334, and SER-122 whereas the protonated nitrogen in the quinoline moiety of compound **4** forms a hydrogen bond with the oxygen of the carbonyl group in HIS-440. In addition, two OH- π interactions occur between the hydroxy groups of TYR-334 and SER-122 and the aromatic linker of compound **4**. Finally, both compounds bind to TYR-121 and TRP-279 in the PAS to ILE-287 (b and d).

Interestingly, the naphthalimido moiety of compound **2** is situated between amino acids PHE-330 and TRP-84 through π - π stacking, whereas the two carbonyl groups are involved in hydrogen bonds with hydroxy groups of residues amino acids ASP-72, TYR-334 (3.2 and 1.9 Å, respectively) and SER-122 (2.5 Å) (Figure 4a). In contrast, the molecular modelling studies reported by Gao *et al.* on their ranitidine derivatives bearing naphthalimido moieties demonstrated strong interactions of the latter structure with the residue TRP-286 of mouse AChE, equivalent to *tc*AChE, TRP-279 at the entrance of the gorge, in the PAS of the AChE^{17,38}. Furthermore, hydrogen bonds are established between the phenolic group of the phenolic moiety and the carbonyl group of ILE-287 (2.7 Å) and between the nitrogen and the hydroxy group of TYR-121 (2.1 Å).

Finally, hydrophobic interactions between the phenolic moiety and TRP-279 are apparent (Figure 4b). Similarly, the tacrine moiety of compound **4** is stacked between PHE-330 and TRP-84. However, the charged nitrogen of tacrine provides a cation- π interaction with TRP-84, whereas the protonated nitrogen in the quinoline ring establishes a hydrogen bond (2.0 Å) with the carbonyl group of the main chain of HIS-440 (Figure 4c). Two OH- π interactions are established between the hydroxy group of SER-122 and TYR-334 and the aromatic linker of compound **4**. In addition, the phenolic moiety is involved in hydrogen bonding with two amino acids of the PAS (TYR-121, 2.2 Å and TYR-334, 3.8 Å), along with another hydrogen bond with ILE-287 (3.9 Å) and hydrophobic interactions with TRP-279 (Figure 4d).

Inhibition of Self-Mediated $A\beta_{(1-42)}$ Aggregation

$A\beta_{(1-42)}$ amyloid aggregation is a hallmark of AD, contributing to the deposition of extracellular amyloid plaques in the cerebral cortex². The ability of the compounds to inhibit the self-mediated aggregation of amyloid $A\beta_{(1-42)}$ peptide was tested using Thioflavin T (ThT) fluorescence assay³² with some modifications. The assay is based on the enhanced fluorescence of ThT upon binding to amyloid fibrils³⁹. All the compounds were tested at concentration of 10 μ M using a final concentration of $A\beta_{(1-42)}$ peptide of 10 μ M as well. Curcumin was used a positive control. The results are shown in Figure 5.

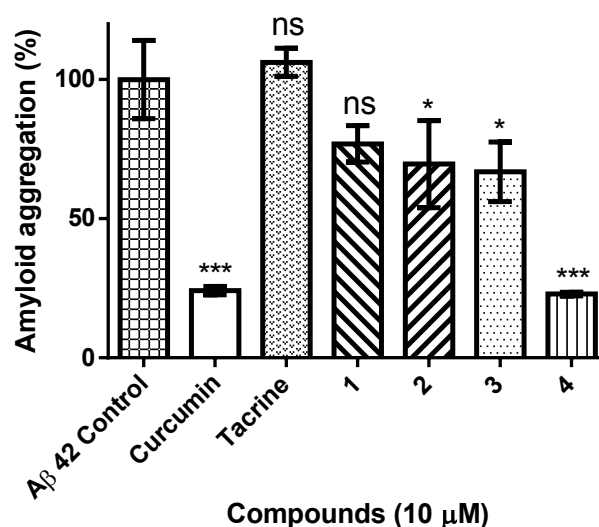


Figure 5. Aggregation inhibitory effects of vanillin derivatives towards amyloid $A\beta_{(1-42)}$ peptide. All the compounds were tested at concentration of 10 μ M. Values are expressed as the percentage of the control and represented as mean \pm SD of three independent experiments in each group. *** p < 0.001, ** p < 0.01, * p < 0.05, ns no significantly different compared to the control.

All compounds showed good to excellent inhibitory properties toward peptide aggregation, with the exception of compound **1**, which showed no significant inhibition compared with the amyloid control. Compounds **2** and **3** showed similar activities, inhibiting $A\beta_{(1-42)}$ peptide aggregation by 30.4 and 33.2%,

respectively. Compound **4** inhibited the $A\beta_{(1-42)}$ peptide aggregation by 77.1% showing similar activity to the positive control curcumin (75.9%) and related tacrine-based derivatives reported by Luo *et al.*³². Interestingly, tacrine alone did not show significant inhibition toward $A\beta_{(1-42)}$ peptide aggregation. The $A\beta_{(1-42)}$ peptide aggregation inhibitory activities of compounds **2**, **3**, and **4** could be explained by the work of Reinke and Gestwicki, which suggested the importance of two aromatic end groups capable of taking part of hydrogen bonding⁴⁰. All of the compounds described in this work bear a hydroxy group in the phenolic moiety that can be involved in hydrogen bonding. However, compound **1** did not show significant $A\beta_{(1-42)}$ peptide aggregation inhibition compared to the control, despite bearing two aromatic end groups and the hydroxy substituent. This may be explained by the length of the linker between the two aromatic end groups, which is shorter in compound **1** compared to compounds **2** and **3** due to the imino double bond. In fact, Reinke and Gestwicki reported that the optimal length of the linker lies between 8 and 16 Å. The length of the linker in compound **1** is 6.9 Å compared to compounds **2**, **3**, **4**, and positive control curcumin (7.3, 7.3, 8.7, and 9.2 Å respectively). Finally, the remarkable activity of compound **4** in this assay could be explained by the presence of the aromatic linker, which confers low flexibility important for the aggregation inhibitory activity⁴⁰. We would like note that all the biological activities observed with our most active compounds are within the same range of activities reported by others working in similar field⁴¹⁻⁴³.

Conclusions

A series of vanillin derivatives was synthesized and found to have similar antioxidant activity to the reference antioxidant, Trolox, except for compound **1**. The results obtained in antioxidant assays agree with our previous study regarding the structure activity relationship for this class of antioxidants¹⁶. Compound **4** displayed the highest antioxidant properties among the vanillin derivatives, showing similar activity to Trolox in DPPH and FRAP assays. However, the latter vanillin derivative turned out to be six times more active than Trolox in the ORAC assay, which is more relevant to the biological systems, involving the use of peroxy free radicals. To date, there has been limited evidence of multi-target-directed ligands with antioxidant activity in ORAC assay as strong as this vanillin derivative for example.⁴⁴ Furthermore, compound **4** exhibited protection of SH-SY5Y cell line against hydrogen peroxide; at concentrations of 5 μM , which turned out to be completely safe in this cell line, the compound reversed peroxide-induced death by 30% after treatment with hydrogen peroxide (400 μM) for 24 hours and showed significant protection at concentration as low as 1 μM . In addition, the compounds showed inhibitory properties toward eel AChE, with IC_{50} ranging from 2.13 to 128.3 μM with the most active compound (**4**) 2-fold less active than the reference agent, tacrine. Computational docking studies suggested that compounds **2** and **4** could bind both the CAS and the PAS of the AChE enzyme through interaction with different

amino acids residues. Although a reduced activity of AChE inhibitory activity was observed with compounds **4**, the overall activity is well compensated by its enhanced antioxidant properties (due to the p-phenylenediamine linker). All the derivatives, except compound **1**, showed inhibitory activities against the self-mediated aggregation of amyloid peptide, with compound **4** being the most active, reducing A β ₍₁₋₄₂₎ peptide aggregation by 77.1% and showing similar activity to curcumin (75.9%). Taken together, the vanillin derivatives reported in this work could provide a viable platform in the development of multi targeted AD therapy.

Experimental section

All the reagents were purchased from Sigma-Aldrich and Fisher Scientific unless otherwise stated. MTT was purchased from ACROS organics. Amyloid A β ₍₁₋₄₂₎ was purchased from Calbiochem. All ¹H and ¹³C spectra were collected using a Magnet Ultrashield Bruker 400 MHz spectrometer. Low-resolution mass spectrometry was performed using Agilent Technologies 1200 series. High-resolution mass spectrometry was performed at EPSRC National Mass Spectrometry Service Centre at Swansea University, Swansea, using Thermo Scientific LTQ Orbitrap XL or Waters Xevo G2-S spectrometers. The progress of each reaction was monitored by thin layer chromatography (TLC aluminium foil silica gel 60 with fluorescence indicator 254 nm, Sigma-Aldrich) through UV light (254-265 nm). Column chromatography was carried out using silica gel (Alfa Aesar 70-230 mesh) as the stationary phase and chloroform/methanol as the mobile phase. The chemical drawing and nomenclature of the compounds were applied according to ChemBioDraw Ultra version 16.0 (CambridgeSoft). Neuroblastoma SH-SY5Y cells were from the European Collection of Authenticated Cell Cultures (ECACC). Cells were maintained at 37 °C (5% CO₂) in DMEM medium (containing GlutaMAX-1 with 25 mM HEPES), supplemented with 10% (v/v) Foetal Bovine Serum (FBS) and 1% Penicillin/Streptomycin (10 mg/mL).

Synthesis of 2-(3-aminopropyl)-1H-benzo[de]isoquinoline-1,3(2H)-dione – I-1

1,8-Naphthalic anhydride (2 g, 10 mmol) was dissolved in ethanol (100 mL); 1,3-Diaminopropane (1.48 g, 20 mmol) was carefully added to the solution and stirred under reflux for 1 hour. The resulting precipitate was filtered and the filtrate concentrated using a rotary evaporator. The solid obtained was washed several times with diethyl ether to give a pale-yellow solid as the product (yield: 56%).

¹HNMR: (CDCl₃ solvent peak δ :7.27), 8.63-7.76 (m, Ar-H, 6H), 4.32-4.29 (t, N-CH₂-CH₂, J = 6.8 Hz, 2H), 2.80-2.77 (t, CH₂-NH₂, J = 5.6 Hz, 2H), 1.95-1.89 (m, CH₂-CH₂-CH₂, J = 13.6 Hz, 2 H), 1.52 (b, NH₂, 2H).

¹³CNMR: (CDCl₃ solvent peak δ : 77.4-76.8) 164.4, 134.0-122.65, 39.48, 37.77, 32.19. LRMS calcd for C₁₅H₁₅N₂O₂ [M+H]⁺ 255.1, *m/z* found 255.0.

Synthesis of 2-(3-((4-hydroxy-3-methoxybenzylidene)amino)propyl)-1H-benzo[de]isoquinoline-1,3(2H)-dione – 1

Vanillin (0.5 g, 3.3 mmol) was dissolved in methanol followed by the addition of 2-(3-aminopropyl)-1H-benzo[de]isoquinoline-1,3(2H)-dione (0.83 g, 3.3 mmol). The reaction was left to stir overnight at RT. The solution obtained was concentrated through rotary evaporation and the solid obtained was dissolved in DCM (25 mL) and extracted 3 times with saturated NaHCO₃ (20 mL). The organic layer was collected and dried with anhydrous sodium sulfate and concentrated through rotary evaporator to afford an orange solid (yield: 73%).

¹HNMR: (CDCl₃ solvent peak δ:7.30), 8.61-6.85 (m, Ar-H, 9H), 8.22 (s, Ar-CH=N, 1H), 4.39-4.35 (t, N-CH₂-CH₂, J = 6.8 Hz, 2H), 3.81 (s, -OCH₃, 3H), 3.79-3.77 (t, CH₂-N=CH, J = 6.8 Hz, 2H), 3.77-3.75 (t, N-CH₂-CH₂, J = 6.8 Hz, 2H), 2.26-2.23 (m, CH₂-CH₂-CH₂, J = 14.0 Hz, 2H). ¹³CNMR: (CDCl₃ solvent peak δ: 77.4-76.7) 164.3, 161-107.8, 59.47, 55.87, 38.95, 29.17. HRMS calcd for C₂₃H₂₁N₂O₄ [M+H]⁺ 389.1497, m/z found 389.1497.

Synthesis of 2-(3-((4-hydroxy-3-methoxybenzyl)amino)propyl)-1H-benzo[de]isoquinoline-1,3(2H)-dione - 2

0.4 g of 2-(3-((4-hydroxy-3-methoxybenzylidene)amino)propyl)-1H-benzo[de]isoquinoline-1,3(2H)-dione (1 mmol) were dissolved in methanol, then 0.057 g of NaBH₄ (1.5 mmol) added. The reaction was stirred for 2 hour and concentrated through rotary evaporation. The solid obtained was dissolved in DCM and extracted 3 times with NaHCO₃ (20 mL). The organic layer was collected and dried with anhydrous sodium sulfate and concentrated through rotary evaporation to afford a pale-yellow solid (yield: 86%). ¹HNMR: (CDCl₃ solvent peak δ:7.31), 8.65-6.82 (m, Ar-H, 9H), 4.34-4.31 (t, N-CH₂-CH₂, J = 7.2 Hz, 2H), 3.91 (s, -OCH₃, 3H), 3.76 (s, Ar-CH₂-N, 2H), 2.78-2.74 (t, CH₂-CH₂-N, J = 6.8 Hz, 2H), 2.05-2.01 (t, CH₂-CH₂-CH₂, J = 6.8 Hz, 2H). ¹³CNMR: (CDCl₃ solvent peak δ: 77.4-76.7) 164.3, 146.61-110.9, 55.9, 53.8, 46.4, 38.3, 28.3. HRMS calcd for C₂₃H₂₃N₂O₄ [M+H]⁺ 391.1652, m/z found 391.1651.

Synthesis of 2-(3-((4-hydroxy-3,5-dimethoxybenzyl)amino)propyl)-1H-benzo[de]isoquinoline-1,3(2H)-dione - 3

Syringaldehyde (0.29g, 1.57 mmol) was mixed with methanol (8 mL) followed by the addition of 2-(3-aminopropyl)-1H-benzo[de]isoquinoline-1,3(2H)-dione (0.40g, 1.57 mmol). The solution was refluxed for 2 hours and left stirring overnight at RT to yield a red solution. The solvent was evaporated under reduced pressure to yield a red solid which was suspended in propan-2-ol followed by the addition of NaBH₄ (3.0 mmol). The solution was refluxed for 48 hours. At the completion of the reaction, the solvent was removed under *vacuo* to afford a solid. The latter was collected by filtration, washed thoroughly with water and methanol to yield the final product (38%) . ¹HNMR: (CDCl₃ solvent peak δ:7.20), 8.53-6.50 (m, Ar-H, 8H),

4.23-4.20 (t, N-CH₂-CH₂, J = 6.8 Hz, 2H), 3.80 (s, -OCH₃, 6H), 3.64 (s, Ar-CH₂-N, 2H), 2.68-2.64 (t, CH₂-N, J = 6.8 Hz, 2H), 1.95-1.91 (t, CH₂-CH₂-CH₂, J = 6.8 Hz, 2H). ¹³CNMR: (CDCl₃ solvent peak δ: 77.4-76.7) 164.3, 147.1-104.9, 56.2, 54.2, 46.5, 38.3, 28.3. HRMS calcd for C₂₄H₂₅N₂O₅ [M+H]⁺ 421.1758, *m/z* found 421.1756.

Synthesis of 9-chloro-1,2,3,4-tetrahydroacridine - **I-2**

Intermediate **I-2** was prepared following the procedure reported in literature ²¹. To a mixture of anthranilic acid (1.85 g, 1.3 mmol) and cyclohexanone (2.6 mL, 2.6 mmol), 15 mL of POCl₃ (0.16 mol) was added in an ice bath. The mixture was heated under reflux and stirred for 24 hours, then cooled and concentrated under reduced pressure. The residue was diluted with ethyl acetate (50 mL), neutralized with saturated Na₂CO₃ (30 mL) and washed 3 times with brine (30 mL). The organic layer was dried and the product was recrystallized from acetone (yield: 67%).

¹HNMR: (CDCl₃ solvent peak δ:7.20), 8.11-7.45 (m, Ar-H, 4H), 3.07-3.04 (t, Ar-CH₂-CH₂, J = 5.2 Hz, 2H), 2.97- 2.94 (t, Ar-CH₂-CH₂, J = 6.4 Hz, 2H), 1.92- 1.84 (m, CH₂-CH₂, 4H). ¹³CNMR: (CDCl₃ solvent peak δ: 77.8-76.7) 159.6- 123.7, 34.3, 27.6, 22.72, 22.68. LRMS calcd for C₁₃H₁₃ClN [M+H]⁺ 218.7, *m/z* found 218.1.

Synthesis of N1-(1,2,3,4-tetrahydroacridin-9-yl)benzene-1,4-diamin - **I-3**

9-chloro-1,2,3,4-tetrahydroacridine (107 mg, 0.5 mmol) was dissolved in 1-pentanol (5 mL) followed by the addition of KI (80 mg, 0.5 mmol) and heated under reflux. Then, p-phenylenediamine (135 mg, 1.25 mmol) was added and the mixture stirred for 24 hours. The solution was concentrated under pressure and the solid obtained dissolved in 50 mL of DCM and extracted 3 times with Na₂CO₃ (50 mL). The organic layer was dried through rotary evaporation and the crude was purified through column chromatography (DCM/MeOH 99:1) to afford a brown solid (yield 39%).

¹HNMR: (CDCl₃ solvent peak δ:7.30), 8.04-6.61 (m, Ar-H, 8H), 5.95 (s, Ar-NH-Ar, 1H), 3.59 (s, Ar-NH₂, 2H), 3.20-3.17 (t, Ar-CH₂-CH₂, J = 6 Hz, 2H), 2.72-2.69 (t, Ar-CH₂-CH₂, J = 6.4 Hz, 2H), 1.98- 1.95 (m, -CH₂-CH₂-, J = 5.6 Hz, 2H), 1.95- 1.89 (m, -CH₂-CH₂-, J = 5.6 Hz, 2H). ¹³CNMR: (CDCl₃ solvent peak δ: 77.4-76.7) 141.7- 116.1, 33.8, 25.2, 24.9, 22.8, 22.7. LRMS calcd for C₁₉H₂₀N₃ [M+H]⁺ 290.2, *m/z* found 290.2.

Synthesis of 2-methoxy-4-(((4-((1,2,3,4-tetrahydroacridin-9-yl)amino)phenyl)amino)methyl)phenol - **4**

I-3 (50 mg, 0.17 mmol) was dissolved in 2-propanol (10 mL) followed by the addition of vanillin (20 mg, 0.13 mmol). The reaction was stirred under reflux and monitored through TLC; when the vanillin spot had disappeared, the solution was cooled down and NaBH₄ (25mg, 0.7 mmol) was added. The solvent was dried

and the solid obtained was purified through column chromatography (DCM/MeOH 99:1) to afford an orange solid (yield 46%).

¹HNMR: (CDCl₃ solvent peak δ:7.19), 8.05-6.50 (m, Ar-H, 11H), 4.14 (s, Ar-CH₂-N, 2H), 3.81 (s, -OCH₃, 3H), 3.13-3.11 (t, Ar-CH₂-CH₂, J = 5.6 Hz, 2H), 2.95-2.93 (t, Ar-CH₂-CH₂, J = 7.2 Hz, 2H), 2.60- 2.56 (m, -CH₂-CH₂-, J = 6.4 Hz, 2H), 1.86- 1.80 (m, -CH₂-CH₂-, J = 12.4 Hz, 2H). ¹³CNMR: (CDCl₃ solvent peak δ: 77.4-76.7) 146.8- 110.3, 56.0, 48.8, 45.82, 25.0, 22.7, 22.3. HRMS calcd for C₂₇H₂₈N₃O₂ [M+H]⁺ 426.2176, *m/z* found 426.2172.

DPPH Assay

The ability of the compounds to scavenge DPPH free radical was determined following the procedure reported by Payet, Sing and Smadja with some modifications in a 96-well set-up²². A dilution series of antioxidants ranging from 1.5 to 750 μM was made in Eppendorf® tubes, then 50 μL were transferred to the corresponding well, while 50 μL of vehicle (methanol) were used as negative control wells. 100 μL of DPPH solution (0.1 mM) were added to each well followed by incubation in the dark for 30 min. Absorbance was then measured at 517 nm using a Bio-Rad iMark microplate reader.

FRAP Assay

The reducing properties of the compounds was tested through the FRAP assay following the method described by Firuzi *et al.* with minor modifications in a 96-well plate²³. FRAP reagent was prepared by mixing 2.5 mL of 10 mM TPTZ (in 40 mM HCl) with 2.5 mL of 20 mM FeCl₃ (in deionized water) and the volume brought to 30 mL with 300 mM sodium acetate buffer (pH 3.6). A dilution series of antioxidants and Trolox ranging from 500 to 5000 μM was made in Eppendorf® tubes, then 10 μL of each was pipetted in the corresponding well in a 96 well-plate along with 190 μL of FRAP reagent. The plate was stored in the dark for 30 minutes before the absorbance was measured at 593 nm using a Bio-Rad iMark microplate reader.

ORAC Assay

The ability of the compounds to prevent oxidative degradation of fluorescein was measured using ORAC assay following the previously protocols reported with minor modifications on a black-walled 96-well plate^{16,22,45}.

A dilution series of antioxidants and Trolox was made in phosphate buffer (75 mM, pH 7.4) in Eppendorf® tubes and 25 μL of each was transferred into the corresponding well whereas 25 μL of phosphate buffer was added in the control wells.

150 μL of 25 nM sodium fluorescein solution was added in each well and the plate was incubated at 37°C for 30 minutes.

Finally, 25 μL of 0.15 M AAPH solution was added in the positive control and in the antioxidant wells whereas 25 μL of phosphate buffer was added in the fluorescein control.

The fluorescence was measured every 2 minutes over a period of 2 hours (485/20 nm excitation, 525/20 nm emission) using a BioTek Synergy HT microplate reader.

MTT Assay

Cell survival after treatment with H_2O_2 (400 μM) was assessed using the MTT cell assay, using a procedure similar to previous publications^{16,46}. SH-SY5Y cells were seeded (7000 cells/well) in a 96-well plate. After adhesion (24 h), cells were treated with different concentrations of compound **4**, ranging from 0.01 to 5 μM , and incubated for 24 h.

Subsequently H_2O_2 solution was added to the positive control and the test drug wells, followed by incubation for another 24 h. After incubation, all the solutions were removed from all the wells and 100 μL of MTT solution (1 mg/mL) was added in each well. The plate was wrapped in aluminum foil and incubated for 4 h at 37 $^\circ\text{C}$.

The solutions in each well were removed by pipette and 100 μL of DMSO added to each well to dissolve the formazan crystals. The plates were gently shaken for 20 minutes and the absorbance measured at 490 nm with a Bio-Rad iMark microplate reader. Cell viability was expressed as a percentage of the absorbance from control cells.

AChE Inhibition Assay

The inhibitory properties of compounds toward AChE was determined through Ellman method with some modifications³⁰. A 22 U/mL stock solution of AChE from *Electrophorus electricus* was prepared in 20 mM tris HCl pH 7.5 and diluted 1/100 before use. A 3 mM (5,5'-dithiobis-(2-nitrobenzoic acid)) solution was prepared by dissolving 0.1189 g of DTNB in 0.05 M phosphate/ 0.09 M hepes buffer (pH 7.5). A 15 mM acetylthiocholine iodide solution was prepared by dissolving 0.1084 g of compound in deionized water. A dilution series of compounds (in methanol) was made in Eppendorf® tubes and 25 μL of the latter was pipetted in the corresponding well in a 96-well plate along with 125 μL of DTNB solution and 25 μL of diluted AChE solution. 25 μL of methanol were added in the control wells. The plate was incubated for 10 minutes at 37 $^\circ\text{C}$ then 25 μL of acetylthiocholine iodide solution were added to each well and incubated for another 10 minutes. The absorbance was measured at 415 nm using a Bio-Rad iMark microplate reader.

Molecular Modelling

For the docking procedure, the pdb structure of 2CMF (*Torpedo californica* AChE in complex with a bis-tacrine linked by a five-carbon spacer) was taken from Protein Data Base (<http://www.rcsb.org>). The choice of the TcAChE instead of an *electrophoresus electricus* model of AChE (which was employed for the

Ellman assay) was based on the good resolution of the structure (2.5 Å), the similarity of the ligand in the structure with compound **4** and the unavailability of high resolution *eeAChE* structures⁴⁷. It is worth noting the high degree of identity between *TcAChE* and *EeAChE*⁴⁸. Water molecules and the original ligand were removed from the protein structure and polar hydrogens and charges were added. The protein was saved as pdbqt file. The 3D structures of compounds **2** and **4** were built using ChemDraw 16.0 (Cambridgesoft, Waltham, MA) and Chem3D Ultra 16 version (Cambridgesoft, Waltham, MA) and its MM2 force field energy minimization tool. The structures were saved as pdb file. The ligands and the macromolecule were then loaded into AutoDock Vina 1.1.2 (Molecular graphics laboratory, The Scripps research group, La Jolla, CA) and prepared for docking. Docking was performed on a grid box (40x40x40 Å) centered on the active site of AChE (residue TRP-84). The lowest energy conformation of each ligand enzyme complex was selected for analyzing the interactions between AChE and the inhibitor and the results were visualized using PyMOL (the PyMOL Molecular Graphics System, Version 2.0.7 Schrödinger, LLC).

ThT Assay

The ability of the compounds to inhibit self-mediated amyloid A $\beta_{(1-42)}$ aggregation was determined through the fluorometric ThT assay following the method described by Luo *et al.* with some modifications³². A 500 μ M stock solution of amyloid A $\beta_{(1-42)}$ peptide was prepared by dissolving 0.25 mg of the peptide in 110 μ L of DMSO. The solution was aliquoted in Eppendorf tubes and stored at -20°C.

Briefly, 2 μ L of peptide solution was pipetted in 96 μ L of 10 mM phosphate/ 10 mM NaCl buffer (pH 8) along with 2 μ L of inhibitor solution (dissolved in DMSO) or 2 μ L of DMSO (for the control). The final concentrations of both the amyloid peptide and inhibitors were 10 μ M. The solutions were incubated for 24 hours at 37°C. Then, 300 μ L of 50 mM glycine/ NaOH buffer (pH 8.5) containing 5 μ M of ThT was added to all the samples.

Each solution was transferred into a cuvette and the fluorescence was measured using a Perkin Elmer LS55 luminescence spectrometer (excitation 446 nm, emission 490 nm).

Statistical Analysis

Data are shown as mean \pm standard deviation (SD) and all the experiments were conducted on at least 3 separate occasions. Statistical analysis was performed using GRAPH PAD prism (6.00 for Windows, GraphPad Software, La Jolla California USA, www.graphpad.com) using ONE WAY ANOVA and Bonferroni's multiple comparison test. Significant differences are labelled accordingly (ns - not significant, $p < 0.05^*$, $p < 0.01^{**}$, $p < 0.001^{***}$).

Conflicts of interest

There are no conflicts of interest to declare

View Article Online
DOI: 10.1039/C9MD00048H

Acknowledgments

The authors would like to thank the Robert Gordon University for financial support (studentship to MS), the EPSRC UK National Mass Spectrometry Service Centre at Swansea University, Swansea, UK for the HR mass spectral analysis and Professor Andrey Shiryaev (Samara Technical University, Russia) for his advice with the molecular modelling analysis.

References

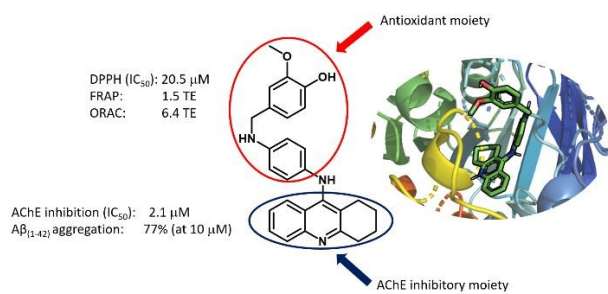
1. Ballard C, Gauthier S, Corbett A, Brayne C, Aarsland D and Jones E. Alzheimer's disease. *Lancet* [Internet]. 2011;377(9770):1019–31. Available from: [http://dx.doi.org/10.1016/S0140-6736\(10\)61349-9](http://dx.doi.org/10.1016/S0140-6736(10)61349-9)
2. Casey DA, Antimisiaris D and O'Brien J. Drugs for Alzheimer's disease: are they effective? *P T*. 2010;35(4):208–11.
3. Alzheimer's association. 2015 Alzheimer's disease facts and figures. *Alzheimer's Dement* [Internet]. 2015;11(3):332–84. Available from: <http://dx.doi.org/10.1016/j.jalz.2015.02.003>
4. Carreiras MC, Mendes E, Perry MJ, Francisco AP and Marco-Contelles J. The Multifactorial Nature of Alzheimer's Disease for Developing Potential Therapeutics. *Curr Top Med Chem* [Internet]. 2013;13(15):1745–70. Available from: <http://www.eurekaselect.com/openurl/content.php?genre=article&issn=1568-0266&volume=13&issue=15&spage=1745>
5. Rosini M, Simoni E, Bartolini M, Tarozzi A, Matera R, Milelli A, Hrelia P, Andrisano V, Bolognesi ML and Melchiorre C. Exploiting the lipoic acid structure in the search for novel multitarget ligands against Alzheimer's disease. *Eur J Med Chem* [Internet]. 2011;46(11):5435–42. Available from: <http://dx.doi.org/10.1016/j.ejmech.2011.09.001>
6. Singh M, Kaur M, Chadha N and Silakari O. Hybrids: a new paradigm to treat Alzheimer's disease. *Mol Divers*. 2016;20(1):271–97.
7. Cavalli A, Bolognesi ML, Minarini A, Rosini M, Tumiatti V, Recanatini M and Melchiorre C. Multi-target-directed ligands to combat neurodegenerative diseases. *J Med Chem*. 2008;51(3):347–72.
8. De Simone A, Bartolini M, Baschieri A, Apperley KYP, Chen HH, Guardigni M, Montanari S, Koblrova T, Soukup O, Valgimigli L, Andrisano V, Keillor JW, Basso M and Milelli A. Hydroxy-substituted trans-cinnamoyl derivatives as multifunctional tools in the context of Alzheimer's disease. *Eur J Med Chem* [Internet]. 2017;139:378–89. Available from: <http://dx.doi.org/10.1016/j.ejmech.2017.07.058>
9. Muñoz-Torrero D. Multitarget Anti-Alzheimer Hybrid Compounds: Do They Work In Vivo? [Internet]. *Design of Hybrid Molecules for Drug Development*. Elsevier Ltd; 2017. 167-192 p. Available from: <http://dx.doi.org/10.1016/B978-0-08-101011-2.00006-4>
10. Liu Q, Qiang X, Li Y, Sang Z, Li Y, Tan Z and Deng Y. Design, synthesis and evaluation of chromone-2-carboxamido-alkylbenzylamines as multifunctional agents for the treatment of Alzheimer's disease. *Bioorganic Med Chem* [Internet]. 2015;23(5):911–23. Available from: <http://dx.doi.org/10.1016/j.bmc.2015.01.042>

11. Fernández-Bachiller MI, Pérez C, González-Muñoz GC, Conde S, López MG, Villarroya M, García AG and Rodríguez-Franco MI. Novel tacrine-8-hydroxyquinoline hybrids as multifunctional agents for the treatment of Alzheimers disease, with neuroprotective, cholinergic, antioxidant, and copper-complexing properties. *J Med Chem*. 2010;53(13):4927–37. Article Online
DOI: 10.1039/C9MD00048H
12. Summers WK, Majovski LV, Marsh GM, Tachiki K and Kling A. Oral Tetrahydroaminoacridine in Long-Term Treatment of Senile Dementia, Alzheimer Type. *N Engl J Med*. 1986;315(20):1241–5.
13. de la Lastra CA and Villegas I. Resveratrol as an antioxidant and pro-oxidant agent: mechanisms and clinical implications. *Biochem Soc Trans [Internet]*. 2007;35(5):1156–60. Available from: <http://biochemsoctrans.org/lookup/doi/10.1042/BST0351156>
14. Jeřábek J, Uliassi E, Guidotti L, Korabečný J, Soukup O, Sepsova V, Hrabínova M, Kuca K, Bartolini M, Pena-Altamira LE, Petralla S, Monti B, Roberti M and Bolognesi ML. Tacrine-resveratrol fused hybrids as multi-target-directed ligands against Alzheimer's disease. *Eur J Med Chem*. 2017;127:250–62.
15. Nepovimova E, Korabecny J, Dolezal R, Babkova K, Ondrejicek A, Jun D, Sepsova V, Horova A, Hrabínova M, Soukup O, Bukum N, Jost P, Muckova L, Kassa J, Malinak D, Andrs M and Kuca K. Tacrine-Trolox Hybrids: A Novel Class of Centrally Active, Nonhepatotoxic Multi-Target-Directed Ligands Exerting Anticholinesterase and Antioxidant Activities with Low in Vivo Toxicity. *J Med Chem*. 2015;58(22):8985–9003.
16. Scipioni M, Kay G, Megson I and Kong Thoo Lin P. Novel vanillin derivatives: Synthesis, anti-oxidant, DNA and cellular protection properties. *Eur J Med Chem [Internet]*. 2018;143:745–54. Available from: <http://linkinghub.elsevier.com/retrieve/pii/S0223523417309753>
17. Gao J, Midde N, Zhu J, Terry A V., McInnes C and Chapman JM. Synthesis and biological evaluation of ranitidine analogs as multiple-target-directed cognitive enhancers for the treatment of Alzheimer's disease. *Bioorganic Med Chem Lett [Internet]*. 2016;26(22):5573–9. Available from: <http://dx.doi.org/10.1016/j.bmcl.2016.09.072>
18. Colvin MT, Silvers R, Ni QZ, Can T V., Sergeyev I, Rosay M, Donovan KJ, Michael B, Wall J, Linse S and Griffin RG. Atomic Resolution Structure of Monomorphic A β 42 Amyloid Fibrils. *J Am Chem Soc*. 2016;138(30):9663–74.
19. Cheung J, Rudolph MJ, Burshteyn F, Cassidy MS, Gary EN, Love J, Franklin MC and Height JJ. Structures of human acetylcholinesterase in complex with pharmacologically important ligands. *J Med Chem*. 2012;55(22):10282–6.
20. Noro J, Maciel J, Duarte D, Olival ACD, Baptista C, Silva ACD, Alves MJ and Kong Thoo Lin P. Evaluation of New Naphthalimides as Potential Anticancer Agents against Breast Cancer MCF-7, Pancreatic Cancer BxPC-3 and Colon Cancer HCT- 15 Cell Lines. *Org Chem Curr Res [Internet]*. 2015;4(3):1–11.
21. Szymański P, Zurek E and Mikiciuk-Olasik E. New tacrine-hydrazinonicotinamide hybrids as acetylcholinesterase inhibitors of potential interest for the early diagnostics of Alzheimer's disease.

- Pharmazie. 2006;61(4):269–73.
22. Payet B, Sing ASC and Smadja J. Assessment of antioxidant activity of cane brown sugars by ABTS and DPPH radical scavenging assays: Determination of their polyphenolic and volatile constituents. *J Agric Food Chem*. 2005;53(26):10074–9.
23. Firuzi O, Lacanna A, Petrucci R, Marrosu G and Saso L. Evaluation of the antioxidant activity of flavonoids by “ferric reducing antioxidant power” assay and cyclic voltammetry. *Biochim Biophys Acta - Gen Subj*. 2005;1721(1–3):174–84.
24. Isa NM, Abdelwahab SI, Mohan S, Abdul AB, Sukari MA, Taha MME, Syam S, Narrima P, Cheah SC, Ahmad S and Mustafa MR. In vitro anti-inflammatory, cytotoxic and antioxidant activities of boesenbergin A, a chalcone isolated from *Boesenbergia rotunda* (L.) (fingerroot). *Brazilian J Med Biol Res*. 2012;45(6):524–30.
25. Rodríguez-Franco MI, Fernández-Bachiller MI, Pérez C, Hernández-Ledesma B and Bartolomé B. Novel tacrine-melatonin hybrids as dual-acting drugs for alzheimer disease, with improved acetylcholinesterase inhibitory and antioxidant properties. *J Med Chem*. 2006;49(2):459–62.
26. Nimse SB and Pal D. Free radicals, natural antioxidants, and their reaction mechanisms. *RSC Adv*. 2015;5(35):27986–8006.
27. DeLange RJ and Glazer AN. Phycoerythrin fluorescence-based assay for peroxy radicals: A screen for biologically relevant protective agents. *Anal Biochem*. 1989;177(2):300–6.
28. Cao G, Alessio HM and Cutler RG. Oxygen-radical absorbance capacity assay for antioxidants. *Free Radic Biol Med*. 1993;14(3):303–11.
29. Kim GH, Kim JE, Rhie SJ and Yoon S. The Role of Oxidative Stress in Neurodegenerative Diseases. *Exp Neurobiol* [Internet]. 2015;24(4):325. Available from: <https://synapse.koreamed.org/DOIx.php?id=10.5607/en.2015.24.4.325>
30. Ellman GL, Courtney KD, Andres V and Featherstone RM. A new and rapid colorimetric determination of acetylcholinesterase activity. *Biochem Pharmacol* [Internet]. 1961;7(2):88–95. Available from: <http://linkinghub.elsevier.com/retrieve/pii/0006295261901459>
31. Chao X, He X, Yang Y, Zhou X, Jin M, Liu S, Cheng Z, Liu P, Wang Y, Yu J, Tan Y, Huang Y, Qin J, Rapposelli S and Pi R. Design, synthesis and pharmacological evaluation of novel tacrine-caffeic acid hybrids as multi-targeted compounds against Alzheimer’s disease. *Bioorganic Med Chem Lett* [Internet]. 2012;22(20):6498–502. Available from: <http://dx.doi.org/10.1016/j.bmcl.2012.08.036>
32. Luo W, Li YP, He Y, Huang SL, Tan JH, Ou TM, Li D, Gu LQ and Huang ZS. Design, synthesis and evaluation of novel tacrine-multialkoxybenzene hybrids as dual inhibitors for cholinesterases and amyloid beta aggregation. *Bioorganic Med Chem* [Internet]. 2011;19(2):763–70. Available from: <http://dx.doi.org/10.1016/j.bmc.2010.12.022>
33. Rydberg EH, Brumshtein B, Greenblatt HM, Wong DM, Shaya D, Williams LD, Carlier PR, Pang YP, Silman I and Sussman JL. Complexes of Alkylene-linked tacrine dimers with *Torpedo californica* acetylcholinesterase: Binding of bis(5)-tacrine produces a dramatic rearrangement in the

- active-site gorge. *J Med Chem.* 2006;49(18):5491–500.
34. Dvir H, Silman I, Harel M, Rosenberry TL and Sussman JL. Acetylcholinesterase: From 3D structure to function. *Chem Biol Interact [Internet].* 2010;187(1–3):10–22. Available from: <http://dx.doi.org/10.1016/j.cbi.2010.01.042>
35. Xu Y, Colletier JP, Weik M, Jiang H, Moulton J, Silman I and Sussman JL. Flexibility of aromatic residues in the active-site gorge of acetylcholinesterase: X-ray versus molecular dynamics. *Biophys J.* 2008;95(5):2500–11.
36. Johnson G and Moore SW. The peripheral anionic site of acetylcholinesterase: structure, functions and potential role in rational drug design. *Curr Pharm Des.* 2006;12(2):217–25.
37. Trott O and Olson A. AutoDock Vina: improving the speed and accuracy of docking with a new scoring function, efficient optimization and multithreading. *J Comput Chem.* 2010;31(2):455–61.
38. Colletier JP, Sanson B, Nachon F, Gabellieri E, Fattorusso C, Campiani G and Weik M. Conformational flexibility in the peripheral site of *Torpedo californica* acetylcholinesterase revealed by the complex structure with a bifunctional inhibitor. *J Am Chem Soc.* 2006;128(14):4526–7.
39. Khurana R, Coleman C, Ionescu-Zanetti C, Carter SA, Krishna V, Grover RK, Roy R and Singh S. Mechanism of thioflavin T binding to amyloid fibrils. *J Struct Biol.* 2005;151(3):229–38.
40. Reinke AA and Gestwicki JE. Structure-activity relationships of amyloid beta-aggregation inhibitors based on curcumin: Influence of linker length and flexibility. *Chem Biol Drug Des.* 2007;70(3):206–15.
41. Panek D, Więckowska A, Pasięka A, Godyń J, Jończyk J, Bajda M, Knez D, Gobec S and Malawska B. Design, Synthesis, and Biological Evaluation of 2-(Benzylamino-2-Hydroxyalkyl)Isoindoline-1,3-Diones Derivatives as Potential Disease-Modifying Multifunctional Anti-Alzheimer Agents. *Molecules.* 2018;23(2):347.
42. Dias KST, de Paula CT, dos Santos T, Souza INO, Boni MS, Guimaraes MJR, da Silva FMR, Castro NG, Neves GA, Veloso CC, Coelho MM, de Melo ISF, Giusti FCV, Giusti-Paiva A, da Silva ML, Dardenne LE, Guedes IA, Pruccoli L, Morroni F, Tarozzi A and Viegas Jr C. Design, synthesis and evaluation of novel feruloyl-donepezil hybrids as potential multitarget drugs for the treatment of Alzheimer's disease. *Eur J Med Chem.* 2017;130:440–57.
43. Benek O, Soukup O, Pasdiorova M, Hroch L, Sepsova V, Jost P, Hrabinoval M, Jun D, Kuca K, Zala D, Ramsay RR, Marco-Contelles J and Musilek K. Design, Synthesis and in vitro Evaluation of Indolotacrine Analogues as Multitarget-Directed Ligands for the Treatment of Alzheimer's Disease. *ChemMedChem.* 2016;11(12):1264–9.
44. Benchekroun M, Romero A, Egea J, León R, Michalska P, Buendía I, Jimeno ML, Jun D, Janockova J, Sepsova V, Soukup O, Bautista-Aguilera OM, Refouvelet B, Ouari O, Marco-Contelles J and Ismaili L. The Antioxidant Additive Approach for Alzheimer's Disease Therapy: New Ferulic (Lipoic) Acid Plus Melatonin Modified Tacrines as Cholinesterases Inhibitors, Direct Antioxidants, and Nuclear Factor (Erythroid-Derived 2)-Like 2 Activators. *J Med Chem.* 2016;59(21):9967–73.

45. Huang D, Ou B, Hampsch-Woodill M, Flanagan JA and Prior RL. High-Throughput Assay of Oxygen Radical Absorbance Capacity (ORAC) Using a Multichannel Liquid Handling System Coupled with a Microplate Fluorescence Reader in 96-Well Format. *J Agric Food Chem* [Internet]. 2002;50:4437–44. Available from: <http://pubs.acs.org/doi/abs/10.1021/jf0201529> New Article Online
DOI: 10.1039/C9MD00048H
46. Goszcz K, Deakin SJ, Duthie GG, Stewart D and Megson IL. Bioavailable Concentrations of Delphinidin and Its Metabolite, Gallic Acid, Induce Antioxidant Protection Associated with Increased Intracellular Glutathione in Cultured Endothelial Cells. *Oxid Med Cell Longev*. 2017;2017:1–17.
47. Ferreira Neto DC, De Souza Ferreira M, Da Conceição Petronilho E, Alencar Lima J, Oliveira Francisco De Azeredo S, De Oliveira Carneiro Brum J, Do Nascimento CJ and Villar JDF. A new guanylhydrazone derivative as a potential acetylcholinesterase inhibitor for Alzheimer's disease: Synthesis, molecular docking, biological evaluation and kinetic studies by nuclear magnetic resonance. *RSC Adv*. 2017;7(54):33944–52.
48. Hebda M, Bajda M, Wieckowska A, Szallaj N, Pasięka A, Panek D, Godyn J, Wichur T, Knez D, Gobec S and Malawska B. Synthesis, molecular modelling and biological evaluation of novel heterodimeric, multiple ligands targeting cholinesterases and amyloid Beta. *Molecules*. 2016;21(4).



Novel vanillin-tacrine hybrid acting as AChE and Aβ₍₁₋₄₂₎ amyloid aggregation inhibitor with strong antioxidant properties enhanced by the *p*-phenylenediamine linker.

Supporting Information (SI)

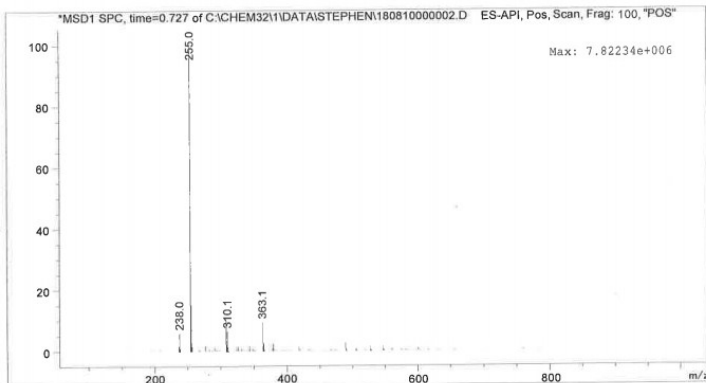
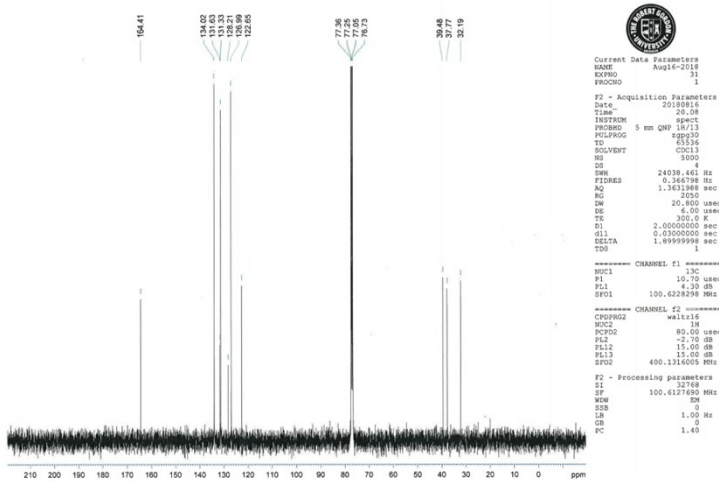
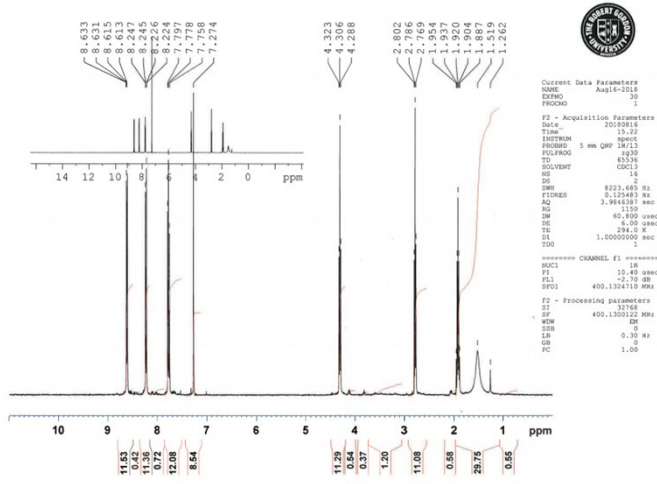
Synthesis of novel vanillin derivatives: novel multi-targeted scaffold ligands against Alzheimer's disease

Matteo Scipioni¹, Graeme Kay¹, Ian L Megson², Paul Kong Thoo Lin*¹

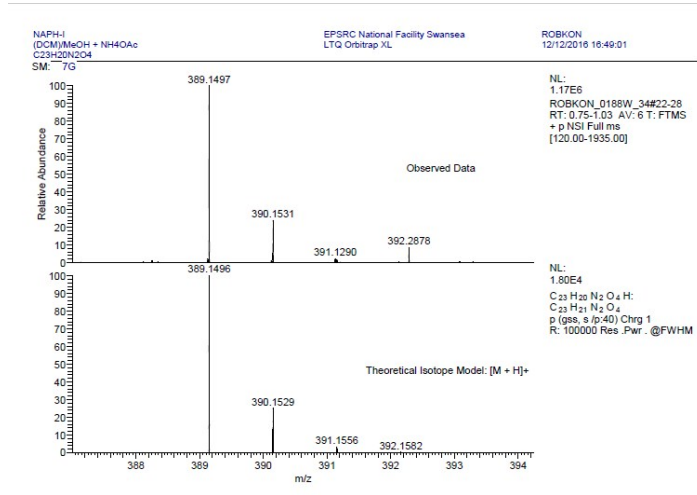
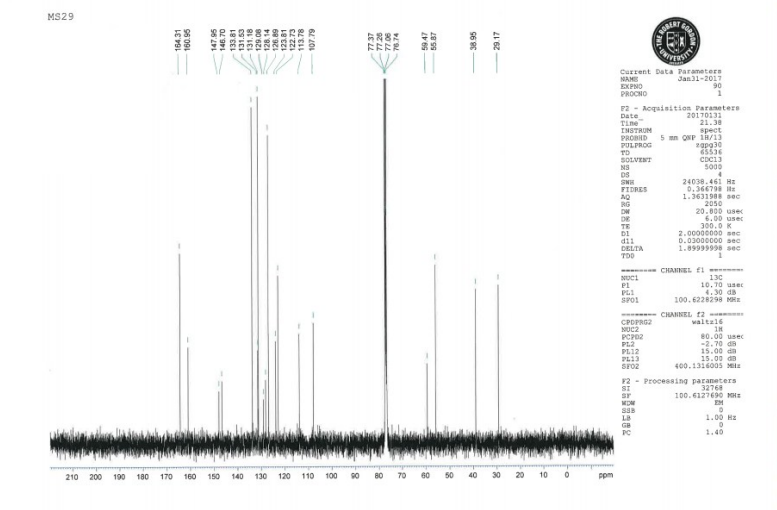
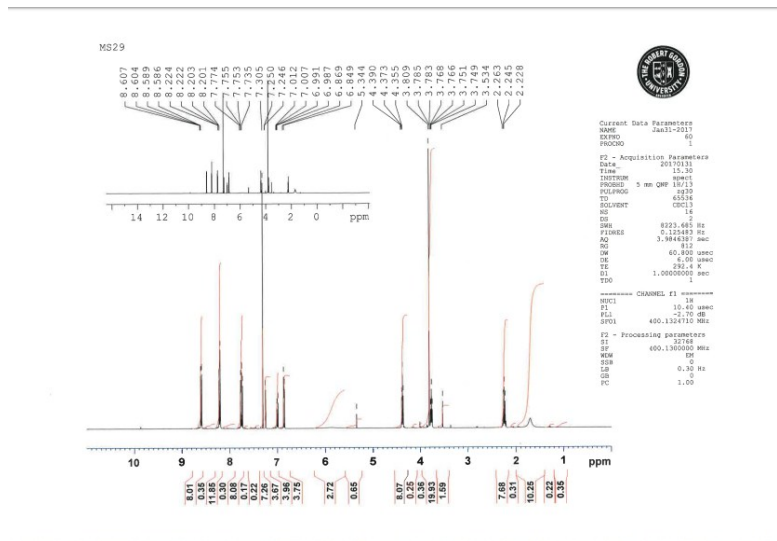
¹*School of Pharmacy and Life sciences, Robert Gordon University, Aberdeen, UK*

²*Institute of Health Research & Innovation, University of the Highlands and Islands, Inverness, UK*

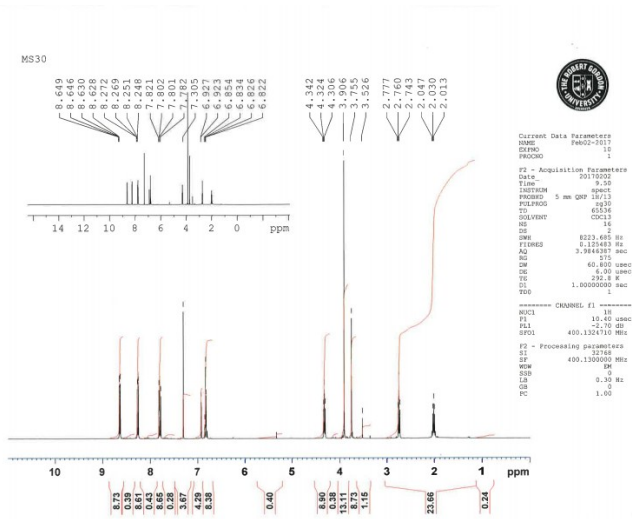
Compound I-1



Compound 1



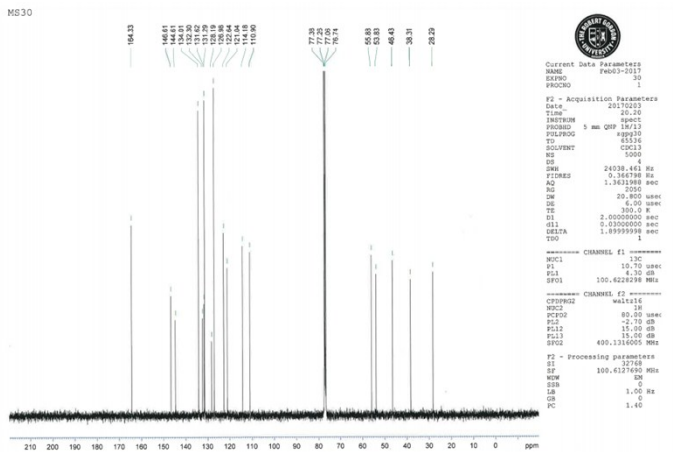
Compound 2



Current Data Parameters
 NAME: Feb02-2017
 EXPNO: 1
 PROCNO: 1
 F2 - Acquisition Parameters
 Date_: 20170202
 Time: 9.32
 INSTRUM: spect
 PROBEHD: 5 mm QNP 1H/13
 PULPROG: zgpg30
 TO: 6233
 SOLVENT: CDCl3
 NS: 16
 DS: 2
 SWH: 8223.685 Hz
 FIDRES: 0.122483 Hz
 AQ: 3.7844387 sec
 SFO: 400.132410 MHz
 SW: 40.800000 MHz
 US: 6.000000 sec
 TE: 295.2 K
 TD: 1.0000000 sec

----- CHANNEL f1 -----
 NUC1: 13C
 P1: 16.40 usec
 PL1: -2.00 dB
 SFO1: 400.132410 MHz

F2 - Processing parameters
 SI: 32768
 SF: 499.1300000 MHz
 WDW: DM
 SSB: 0
 LB: 9.30 Hz
 GB: 0
 PC: 1.00

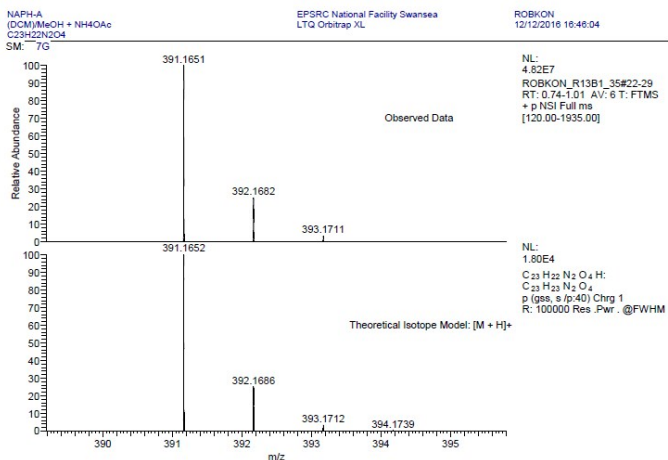


Current Data Parameters
 NAME: Feb02-2017
 EXPNO: 3
 PROCNO: 1
 F2 - Acquisition Parameters
 Date_: 20170202
 Time: 20.20
 INSTRUM: spect
 PROBEHD: 5 mm QNP 1H/13
 PULPROG: zgpg30
 TO: 6233
 SOLVENT: CDCl3
 NS: 5000
 DS: 24938.464 Hz
 SWH: 1.582188 MHz
 FIDRES: 1.631398 sec
 AQ: 700
 SFO: 20.800000 MHz
 US: 6.000000 sec
 TE: 299.0 K
 TD: 2.0000000 sec
 GB1: 0.0300000 sec
 GB2: 1.8999998 sec
 TD0: 1

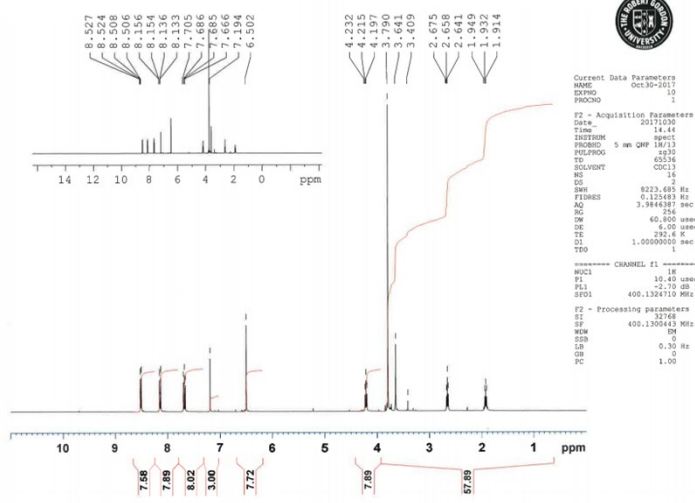
----- CHANNEL f1 -----
 NUC1: 13C
 P1: 16.70 usec
 PL1: 4.30 dB
 SFO1: 100.6228288 MHz

----- CHANNEL f2 -----
 NUC2: 1H
 P2: 62.00 usec
 PL2: -2.70 dB
 PL12: 19.00 dB
 SFO2: 499.1316000 MHz

F2 - Processing parameters
 SI: 32768
 SF: 100.6127690 MHz
 WDW: DM
 SSB: 0
 LB: 1.00 Hz
 GB: 0
 PC: 1.40



Compound 3

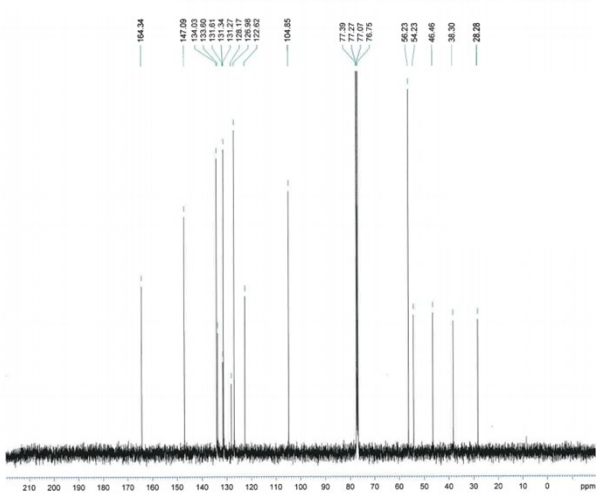


Current Data Parameters
 NAME Oct30-2017
 EXPNO 10
 PROCNO 1

F2 - Acquisition Parameters
 Date_ 20171030
 Time 14:44
 INSTRUM spect
 PROBRD 5 mm QNP 1H/13
 PULPROG zgpg30
 TO 65336
 SOLVENT CDCl3
 NS 16
 DS 2
 SFO1 400.1324110 MHz
 FIDRES 0.120483 Hz
 AQ 3.3846387 sec
 RG 256
 DW 60.800 usec
 DE 6.00 usec
 TE 300.2 K
 TD 1.0000000 sec
 TQ 0

----- CHANNEL f1 -----
 NUC1 13
 P1 10.40 usec
 PL1 -2.50 dB
 SFO1 400.1324110 MHz

F2 - Processing parameters
 SI 32768
 SF 400.130643 MHz
 WDW EM
 SSB 0
 LB 0.30 Hz
 GB 0
 PC 1.00



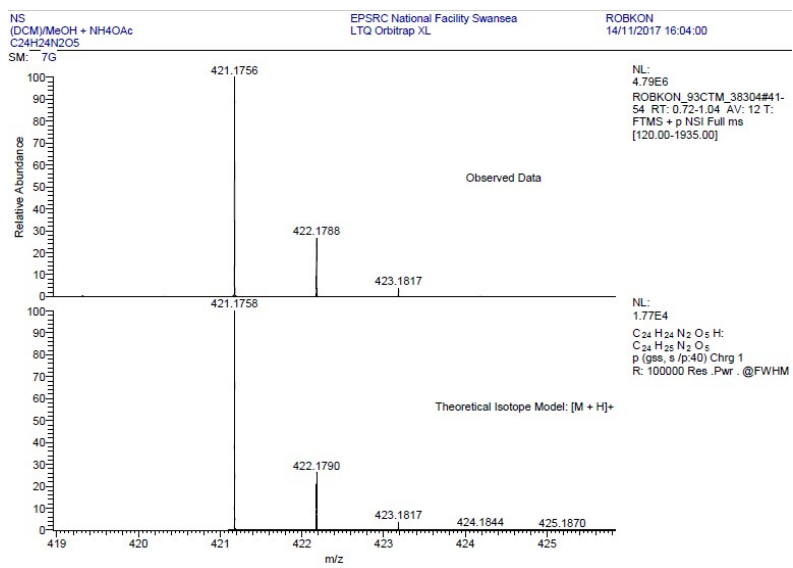
Current Data Parameters
 NAME Oct30-2017
 EXPNO 20
 PROCNO 1

F2 - Acquisition Parameters
 Date_ 20171030
 Time 15:03
 INSTRUM spect
 PROBRD 5 mm QNP 1H/13
 PULPROG zgpg30
 TO 65336
 SOLVENT CDCl3
 NS 1200
 DS 2
 SFO1 400.1324110 MHz
 FIDRES 0.356798 Hz
 AQ 1.3931988 sec
 RG 2560
 DW 20.800 usec
 DE 6.00 usec
 TE 300.2 K
 TD 2.0000000 sec
 TQ 0.3300000 sec
 DELTA 1.8999999 sec
 TQ 0

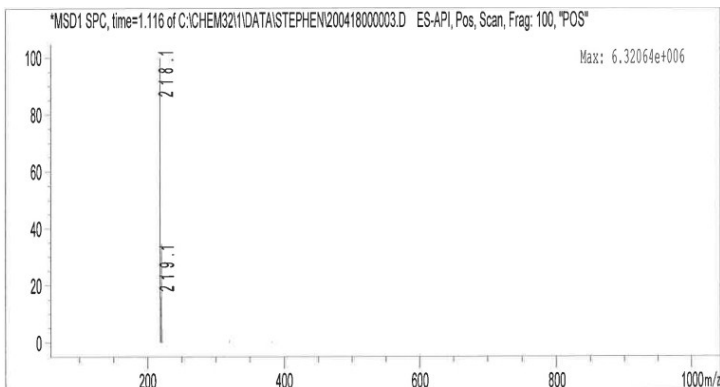
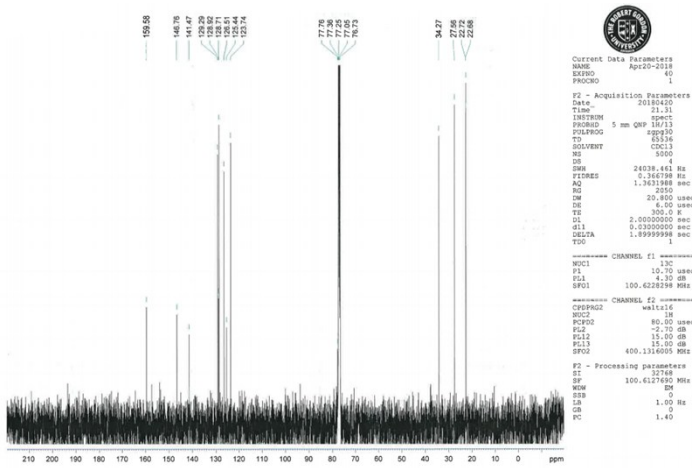
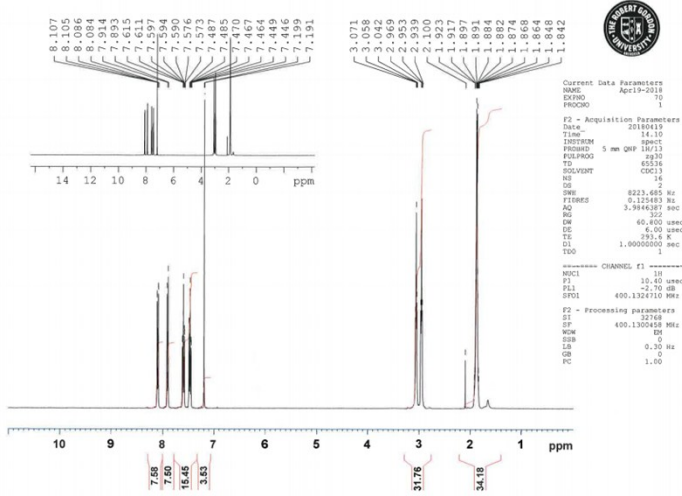
----- CHANNEL f1 -----
 NUC1 13
 P1 10.70 usec
 PL1 -2.50 dB
 SFO1 100.6282498 MHz

----- CHANNEL f2 -----
 CPROG2 waltz16
 NUC2 1H
 P2 65.00 usec
 PL2 -2.70 dB
 PL12 15.00 dB
 PL13 15.00 dB
 SFO2 400.1316059 MHz

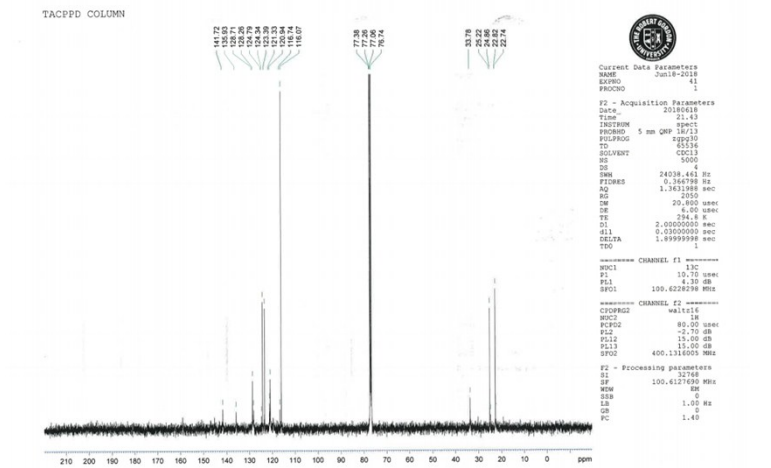
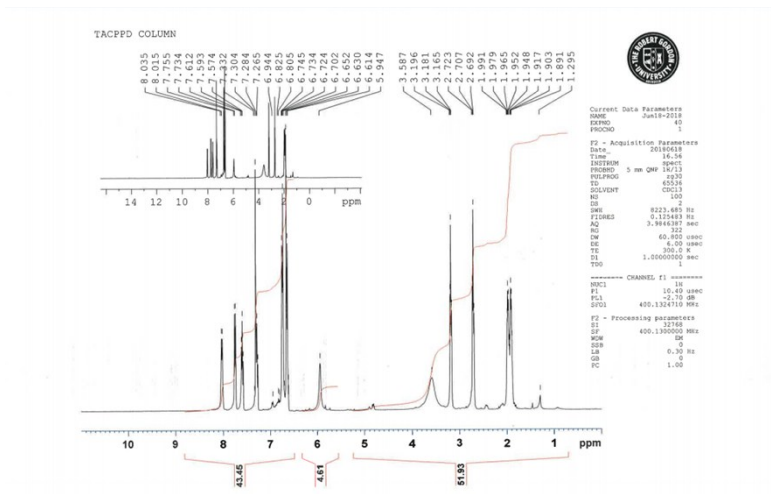
F2 - Processing parameters
 SI 32768
 SF 100.6127680 MHz
 WDW EM
 SSB 0
 LB 1.00 Hz
 GB 0
 PC 1.40



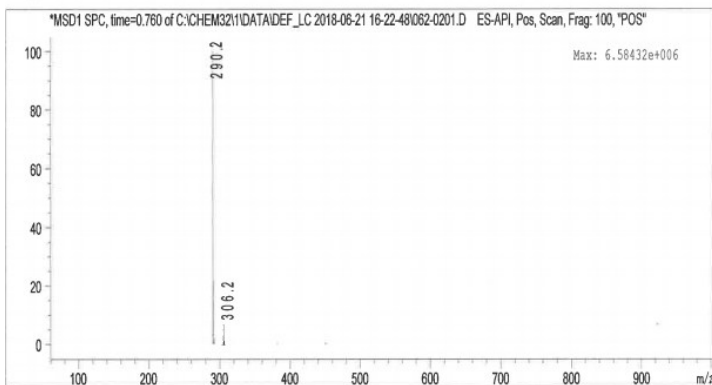
Compound I-2



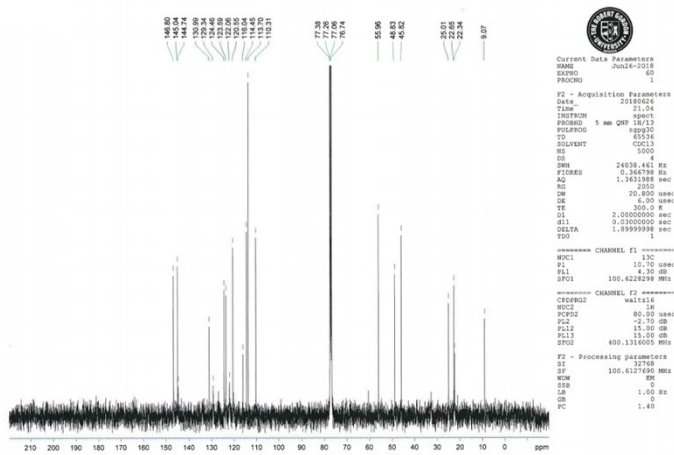
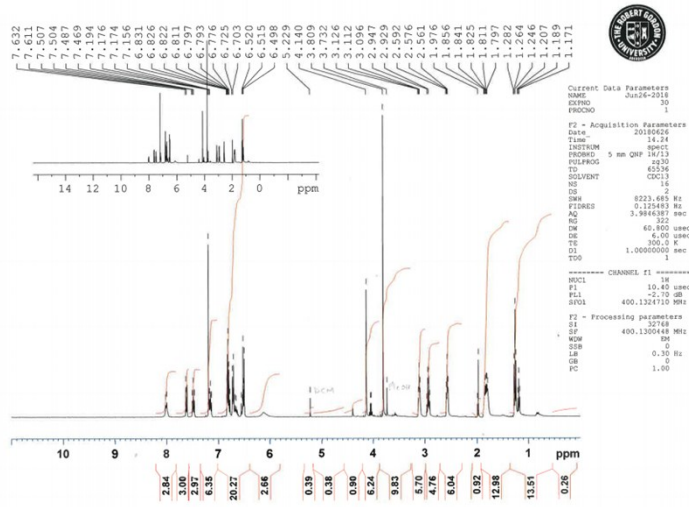
Compound I-3



Tacppd



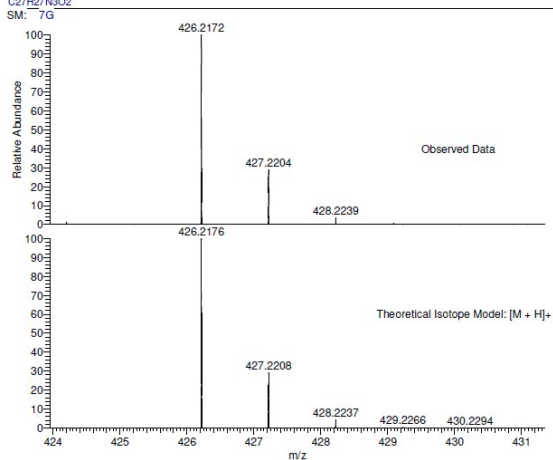
Compound 4



MS41
(MeOH)/MeOH.NH4OAc
C27H27N3O2

EPSC National Facility Swansea
LTO Orbitrap XL

ROBKON
28/09/2018 12:06:37



NL:
7.32E6
ROBKON_93KP9_48091#42-
56 RT: 0.74-1.02 AV: 11 T:
FTMS + p NSI Full ms
[120.00-1935.00]

NL:
1.72E4
C27H27N3O2 H:
C27H28N3O2
p (gss, s [p-4]) Chg 1
R: 100000 Res.Fwhm . @FWHM